FERMILAB-CONF-78-169-E
COO-1428-456

E-344

Review of Non-Annihilation Processes*

V.E. Barnes

Purdue University, Physics Department
West Lafayette, Indiana 47907, U.S.A.

Invited Review Talk to be Published
in the Proceedings of the
IV European Anitproton Conference,
Barr(Strasbourg), France, 1978

Introduction

Hadronic reactions are now known to have many features in common whether the initial particles are mesons or baryons, strange or non-strange, particle or antiparticle. This review of non-annihilation processes is designed to place antiproton-proton interactions in this general hadronic context. An attempt is made to bring out the universal features of hadronic interactions, the better to contrast with unique features of antiproton-proton interactions arising in large part from the annihilation process.

This review will emphasize results from the period since the Stockholm Antiproton Conference, and will emphasize somewhat the higher end of the available range of energies. The topics to be presented include:

1. Total Cross Sections and Cross Sections Differences
2. Elastic Scattering:
   Total; Differential; Real part of forward scattering amplitude; Polarizations
3. Inelastic Single and Double Diffractive Dissociation
4. Charge Exchange Reactions
5. Inclusive Reactions
6. Exclusive Final States
7. Neutral and Strange Particle Production
8. Vector and Tensor Meson Production
9. Symmetries and a General Theorem
10. Applications of the Quark Parton Model to "Soft" Hadronic Processes

*) Work supported in part by the U. S. Department of Energy

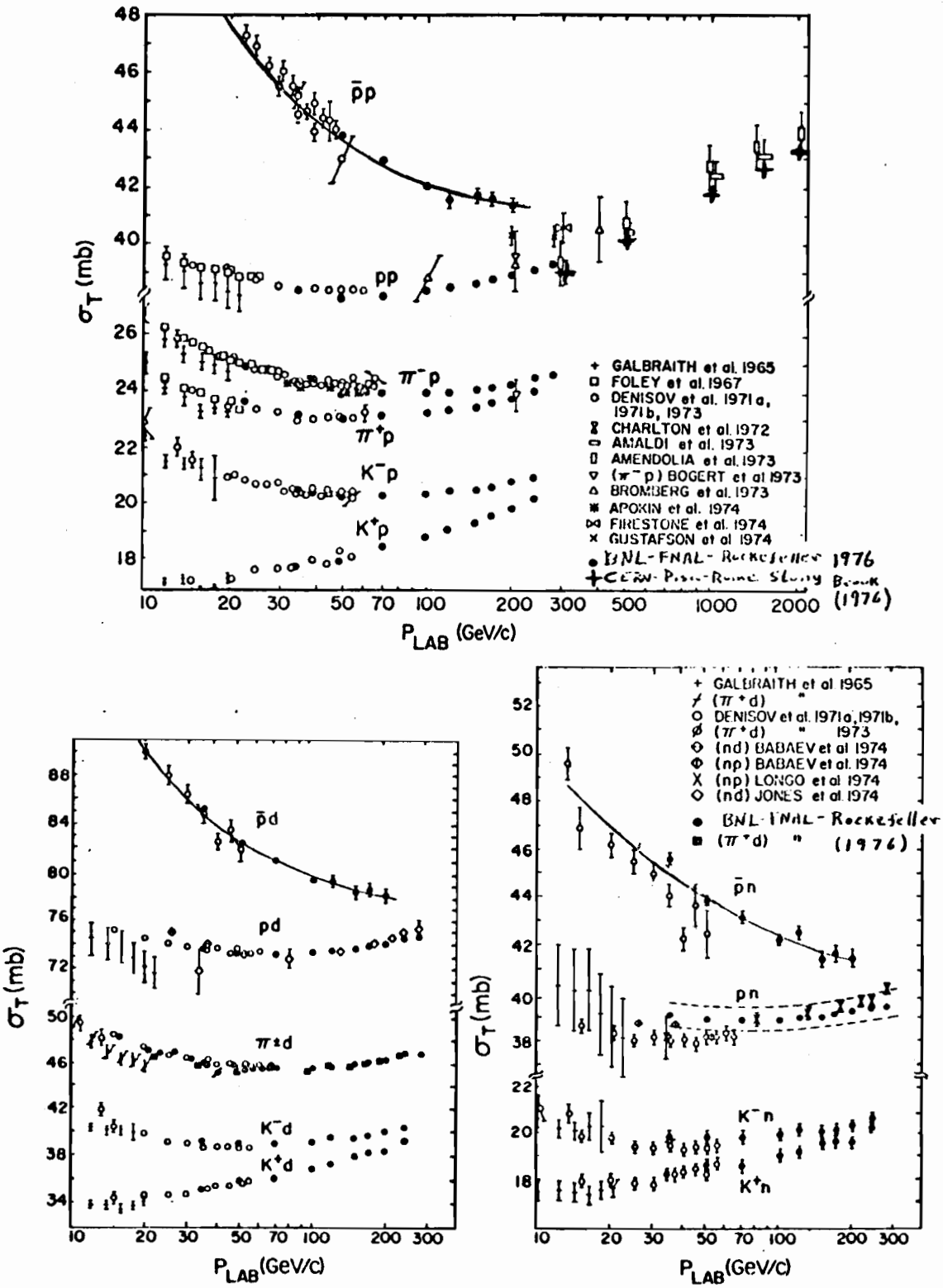

Fig. 1. Total hadron-hadron scattering cross sections as a function of laboratory beam momentum. From Ref. 1 (and from references cited therein). Points from Ref. 5 have been added. Curves have been added to accentuate the $\bar{p}$ data and to guide the eye.

1. Total Cross Sections

Measurements at Fermilab by the BNL-Fermilab-Rockefeller collaboration[1] have extended our knowledge of total cross sections to 280 GeV for pn, K^+N and π^-N; to 240 GeV/c for K^-N and π^+N; and to 200 GeV/c for $\bar{p}N$ (N = n or p). All cross sections except $\bar{p}N$ are rising with energy by this point (Figure 1) and particle-antiparticle cross section differences are decreasing with energy (see also Figure 2) in a remarkably regular way. The authors fit all the data with the simple Regge exchange form $\Delta\sigma = As^{\alpha-1}$ with α in the range 0.38 to 0.41 for ($\bar{p}p$ - pp), ($\bar{p}n$ - pn), (K^-p - K^+p), and (K^-n - K^+n), and $\alpha = 0.55 \pm 0.03$ for (π^-p - π^+p).

As has been noted[2], the total cross section difference $\sigma(\bar{p}p$ -pp) and the $\bar{p}p$ annihilation cross sections which have been measured up to 12 GeV/c both follow the same curve, which has the power law dependence $p_L^{-0.61}$. While this suggests that the difference between the total $\bar{p}p$ and pp cross sections is due to annihilation, Eylon and Harari[3] using arguments based on duality diagram models show that the exchange of meson trajectories contributes to the non-annihilation part of the pp total cross section while the annihilation part is induced by baryon exchange diagrams which sum to give a "Pomeron" contribution with an unexpected power law dependence the same as that for meson exchange. Eylon and Harari predict the same energy dependence but a different magnitude for the annihilation cross section and for the total cross section difference:

$$\Delta\sigma/\sigma_{ANN.} \rightarrow \eta_1 \leq 1 \quad \text{as} \quad s \rightarrow \infty$$

Experimentally $\eta_1 \approx 1$. Another testable prediction of the model involves the topological cross sections for various charged particle multiplicities,

$$\frac{\sigma_n(pp) - \sigma_n(pp)}{\sigma_n(pp)} = \beta^n \, s^{2\alpha_B - 2\alpha_M} - (1 - \eta_1)\, \gamma^n$$

where the exponents α are the intercepts of the exchanged baryon and meson trajectories and $\beta > 1$ and $\gamma < 1$ are constants which in an oversimplified model take the values 3/2 and 1/2. This relationship has been studied at 100 GeV by the Cambridge-FNAL-Michigan State group[4],

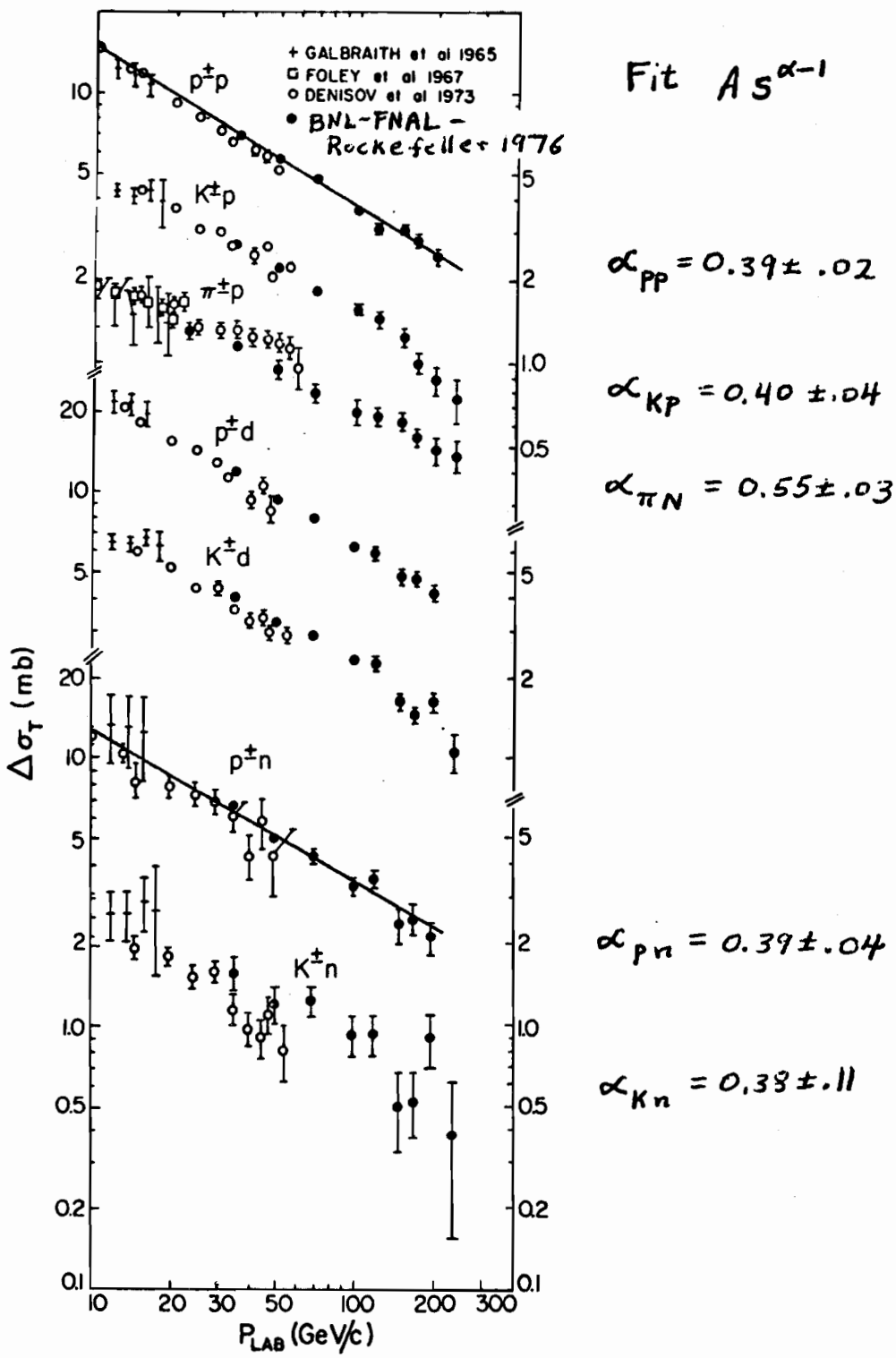

Fit $A s^{\alpha-1}$

$\alpha_{pp} = 0.39 \pm .02$

$\alpha_{Kp} = 0.40 \pm .04$

$\alpha_{\pi N} = 0.55 \pm .03$

$\alpha_{pn} = 0.39 \pm .04$

$\alpha_{Kn} = 0.38 \pm .11$

Fig. 2. Antiparticle - particle total cross section differences as a function of laboratory beam momentum. From Ref. 1 (and from references cited therein). Curves have been added to accentuate the $\bar{p}$ data and to guide the eye.

who find that the second term is indeed near zero as expected for $\eta_1 \approx 1$, and who find that $\beta = 1.24 \pm 0.2$, qualitatively consistent with the predictions of the model and perhaps quantitatively consistent if the exponent n counts produced clusters having charged multiplicity approximately 2.

Coming back to total cross sections, extensive ISR measurements of $\sigma_{tot}(pp)$ with 0.6% accuracy up to $\sqrt{s} = 62.7$ GeV (2000 GeV/c equivalent laboratory momentum)[5] confirm the continued rise of the total cross section (Figure 1) but cannot discriminate between dependences of the form $A + B(\ln(s))^n$ with $n = \frac{1}{2}$, 1, or 2; or the form $A + Bs^{\epsilon}$ which would eventually violate the Froissart bound, $\ln^2(s)$, at high enough energy.

Hendrick at al.[6] have made a phenomenological analysis of a preliminary version of these data, fitting the falling part with Regge exchanges. They obtain intercepts of the ρ and and ω: $\alpha_\rho = 0.57$ and $\alpha_\omega = 0.43$, and find universality of the ω and ρ residues and compatibility with ω - f exchange degeneracy. They fit the rising (Pomeron) part of the cross section using the compact empirical form

$$\sigma_i^{DIFFR}(s) = C_i \ln\left(\frac{s + m_i}{b_i}\right)$$

for particle i on protons, where the coefficients C_i are in the ratios 2:2:3 for π:K:p, thus insuring that the naive SU(3) quark model prediction will hold at asympotic energies, where the expressions will also exhibit ln(s) dependence.

Lipkin[7] has also fitted the total cross section data phenomenologically, using one crude universal $s^{-\frac{1}{2}}$ Regge term plus a two-component Pomeron with p_{lab}^{ϵ} and $p_{lab}^{-\delta}$ energy dependences. The relative magnitudes of the three terms are given by rules involving the numbers of strange and non-strange quarks and antiquarks in the various beam particles, and again one recovers asymptotically the two quark: three quark naive cross section ratio for meson-proton and proton-proton scattering. Lipkin's ansatz of a two component Pomeron is arranged to fit the empirical observation of Denisov et al.[8] that

$$2/3\ \bar{\sigma}(NN) + \bar{\sigma}(KN) = 2\ \bar{\sigma}(\pi N)$$

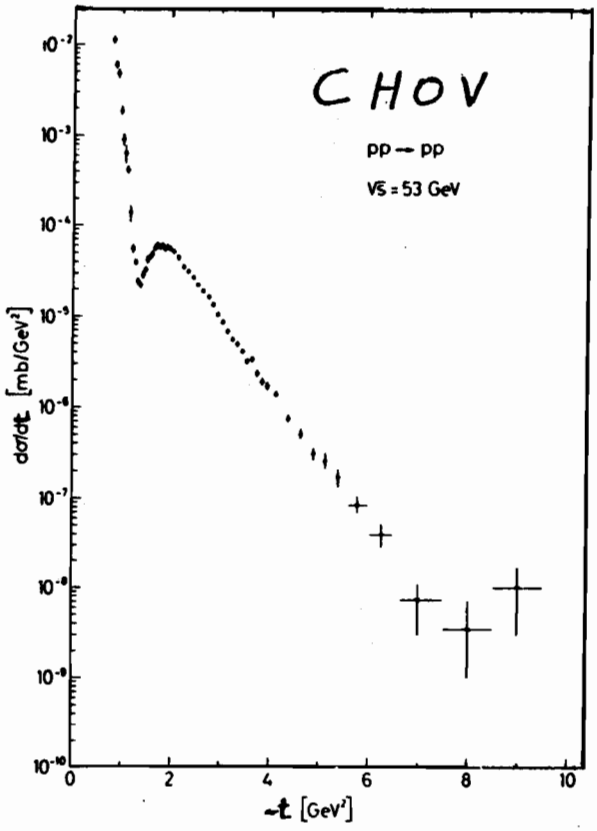

Fig. 3. Differential elastic pp scattering cross section as a function of -t, from Ref. 18.

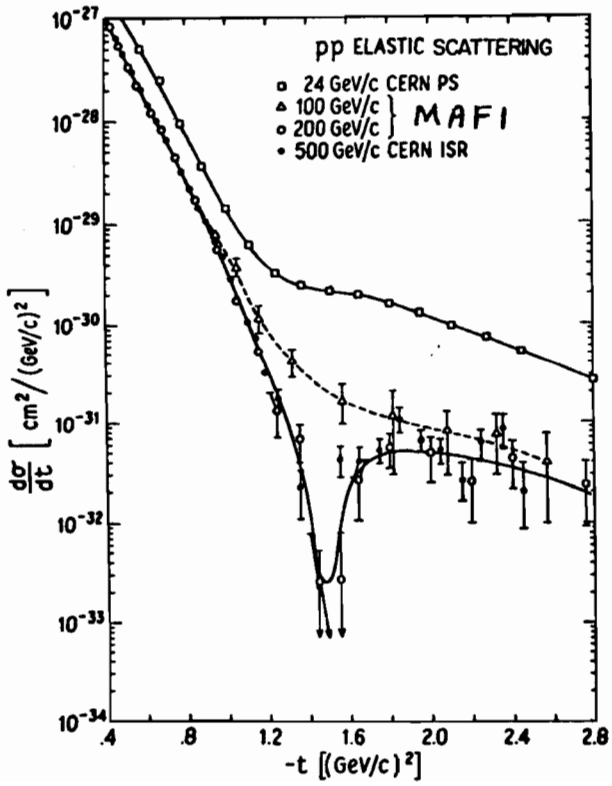

Fig. 4. Differential elastic pp scattering cross section as a function of -t, from Ref. 16 (and from references cited therein).

where $\bar{\sigma}$ is the total cross section averaged over particle and anti-particle and over all isotopic spin components, a relationship which holds to about 2% from 20 GeV up to the highest measured point at 200 GeV.

Hacinliyan and Koca[9] extend the analysis of Lipkin and of Hendrick et al. with a detailed set of Reggeon exchanges plus the two component Pomeron, the latter being fit by universal expressions $A + B\ln(p_L)$ and $p_L^{-0.25}$, with p_L being the incident laboratory momentum. The authors observe that the decreasing Pomeron component looks rather like the f^o trajectory with a high intercept. This is reminiscent of the Pomeron-f identity scheme of Chew and Rosenzweig[10] which has been shown by Stevens, Chew, and Rosenzweig[11] to fit the moderate energy ($p_L < 30$ GeV/c) meson-baryon and baryon-baryon total cross sections, using an intercept $\alpha_o = 0.96$ for the f meson trajectory. However, Duke[12] has shown that this scheme fails badly for vector meson production by meson beams, whereas the standard ω-f exchange degeneracy model is adequate to describe these data.

2. Elastic Scattering

2.1 Total and Differential Elastic Scattering

Recent measurements of elastic scattering have been reported for $\bar{p}p$ below 2.34 GeV/c by a British collaboration[13]; at 8 and 16 GeV for negative hadrons by a CMU-BNL collaboration[14]; for all hadrons $h^{\pm}$ at 39 and 44.5 GeV/c by a Dubna-ITEP-Saclay-Serpukhov collaboration[15]; at 50, 100, and 200 GeV/c by the Michigan-ANL-Fermilab-Indiana group (MAFI)[16]; from 50 to 175 GeV/c by the Fermilab Single Arm Spectrometer Group (FSASG)[17]; and figure 3 shows the results of ISR measurements in the Split Field Magnet Detector by the CERN-Hamburg-Orsay-Vienna group (CHOV)[18] of pp elastic scattering at $\sqrt{s} = 53$ GeV, up to very large momentum transfers $0.8 \leq -t \leq 9$ GeV^2. One sees the well known steep exponential slope at low t, dip in the region $-t \sim 1.2$ to 1.4 GeV^2, secondary maximum, and constant gentler exponential slope with no further structure all the way out to $-t = 9$ GeV^2. The smooth dependence at large t has been observed also for -t between 4.9 and 12.1 GeV^2 in 201 GeV pp elastic scattering, by the Cornell-McGill-North eastern-Lebedev group [19]. Van Hove[20] has fitted these data well

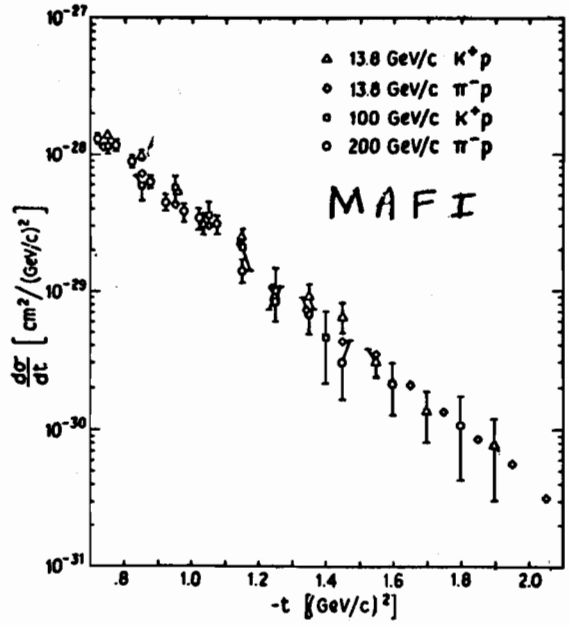

Fig. 5. Differential elastic meson-proton scattering cross sections as a function of -t, from Ref. 16 (and from references cited therein).

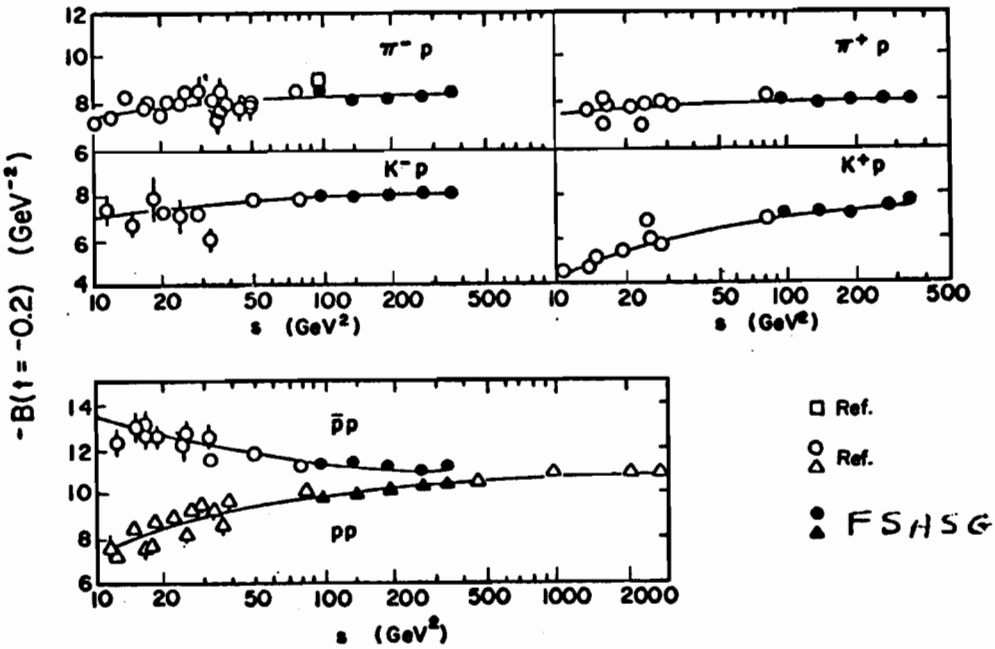

Fig. 6. Exponential elastic slope parameters at -t = 0.2 GeV^2 as a function of s. From Ref. 17 (and from references cited therein).

using a quark-glue model of the hadron in which the glue is taken to be the active constituent in the predominant low p_T part of the hadronic scattering.

The MAFI group[16] find that the 1.4 GeV^2 dip structure is quite pronounced at $p_{LAB} \geq 200$ GeV/c but not at lower energies (Figure 4). Data for $\bar{p}p$ scattering in this range of t are available only up to 45 GeV/c[15] and only up to $-t = 1.4$ GeV^2 so the status of such structure in the $\bar{p}p$ case is unknown. Such structure is certainly absent for meson-proton scattering[16] where the slope decreases gradually up to the highest measured -t, ~ 1.5 to 2 GeV^2. Figure 5 shows a universal behavior of $d\sigma/dt$ for mesons from 13.8 to 300 GeV energy: for $0.8 \leq -t \leq 2.0$ GeV^2 this universal t distribution is very smooth.

The s dependences of the logarithmic t slopes, B, have been measured for all beams by FSASG[17] and are shown (evaluated at $-t = 0.2$ GeV^2) in Figure 6. The values of B are all seen to level off from below with the exception of the $\bar{p}p$ slope which is approaching the pp slope from above. It is probably no coincidence that the $\bar{p}p$ system is also the only one whose total cross section is still decreasing at these energies. The values of B for particle and antiparticle are approaching each other and for mesons seem to be approaching a common value of about 8 GeV^{-2}, while the $p^{\pm}p$ slope may be approaching a value $\sim$10.7 GeV^{-2}.

Structure observed first in pp elastic scattering as a steepening of E by perhaps 2 GeV^{-2} below $-t = 0.15$ GeV^2, may well be common to all hadron proton elastic scattering, as reported by FSASG[21] and reviewed by Lach[22]. It has been traditional to study shrinkage (or anti-shrinkage) of the diffraction peak by evaluating b somewhat above this point.

Elastic cross sections all decrease rapidly with energy and then level off above about 100 GeV/c, as shown in Figure 7. Above about 50 GeV the ratio σ_{el}/σ_{tot} is remarkably constant with energy (Figure 8) and has the value 0.14 for $\pi^{\pm}p$, 0.125 for $K^{\pm}p$, and 0.185 for $p^{\pm}p$, a value approximately 3/2 as large as for meson-proton scattering and close to the ratio 0.185 obtained by Van Hove[23] in a model where elastic scattering arises as the shadow scattering of inelastic processes.

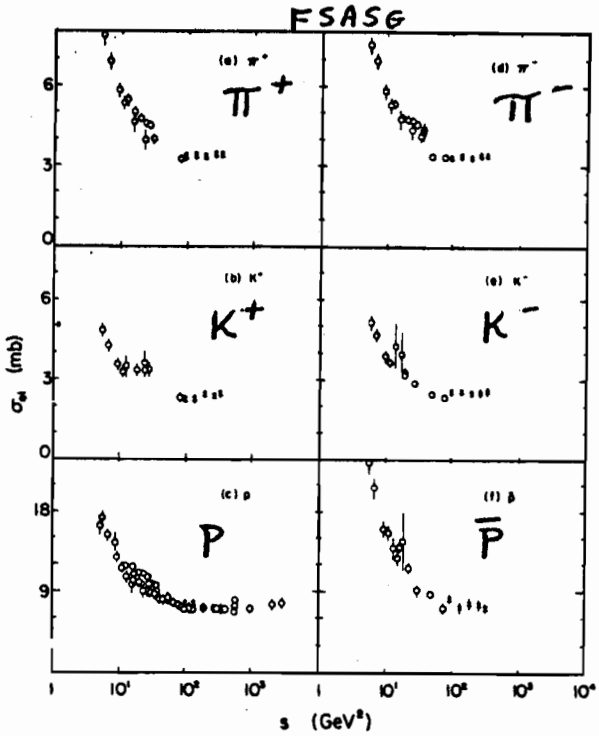

Fig. 7. Elastic cross sections for hadrons on protons, as a function of s. From Ref. 17 (and from references cited therein).

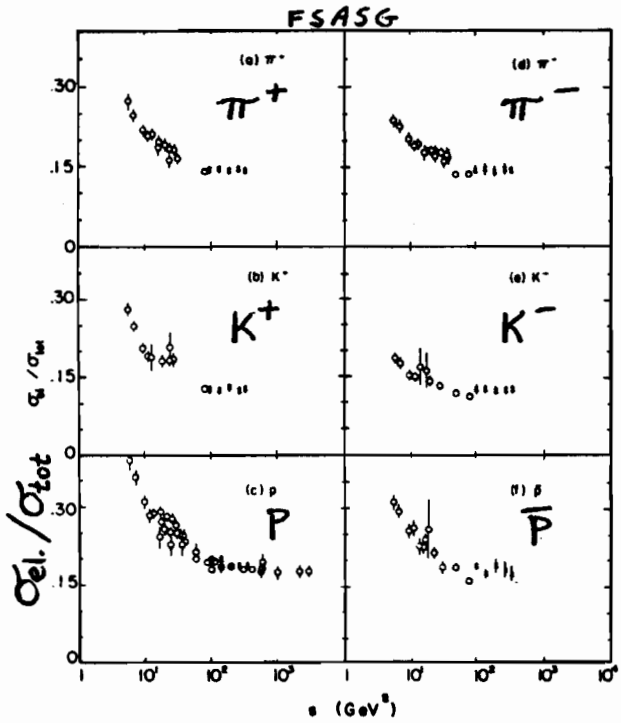

Fig. 8. Ratio of elastic to total cross sections, for hadron-proton scattering, as a function of s. From Ref. 17 (and from references cited therein).

The smallness of the ratio σ_{el}/σ_t is discussed by Bishari[24] in terms of a factorizable dual bootstrap model, and he derives the relation $\sigma_{el}/\sigma_t \simeq 1/N^2$ where N is the effective number of quark flavors. One has $N \approx 2.5$ which may be reasonable in the light of SU(n) symmetry breaking for the strange and heavier quarks.

A good representation of certain regularities in the elastic and total cross sections comes from the hypothesis of geometrical scaling (GS)[25] first used to correlate various pp elastic and total cross section measurements at the ISR. One has that σ_{tot}, σ_{el} and the forward elastic slope parameter B all depend on energy in the same way; hence σ_{el}/σ_{tot} and B/σ_{tot} are independent of energy. Moreover, $(1/\sigma^2_{tot})d\sigma/dt$ plotted against $t\sigma_{tot}$ is predicted to be independent of energy. This scaling is seen in the K^+p data between 70 and 175 GeV (Figure 9) and is well satisfied for the pp data from 175 GeV up to the highest measured ISR energy (Figure 10).

Barger and Phillips[26] have noted an approximate universality of the ratio B^2/σ_T for the Pomeron term in NN, πN, KN, ρN, ωN, and ϕN scattering. The following table compares these quantities at 175 GeV/c for π, K, and p, from the FSASG data:

	$\pi^\pm$	$K^\pm$	$p^\pm$
	2.81 ± .04	2.91 ± .06	2.74 ± 0.3
B^2/σ_{tot}	2.96 ± .04	3.18 ± .08	3.01 ± .10

Universality to ±7% holds for these data. This parameter is more tightly grouped for positive beams, and one would expect that the K^+p and pp systems, with exotic quantum numbers in the s channel, would have the non-Pomeron terms vanishing most quickly with energy.

For details of other features of elastic scattering, including Regge fits to be the s dependence, values of the elastic particle-antiparticle crossovers in $d\sigma/dt$, an impact parameter representation of the differential cross section, and quark model relations in the spirit of Lipkin's two-component Pomeron, the reader is referred to the FSASG papers[17].

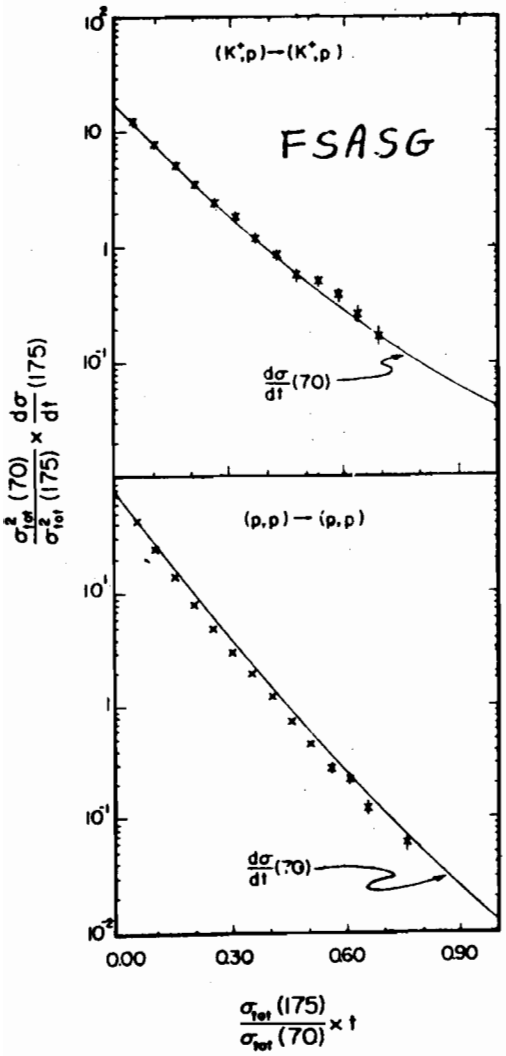

Fig. 9. Geometrical-scaling test for K^+p and pp differential cross sections between 70 and 175 GeV/c. From Ref. 17.

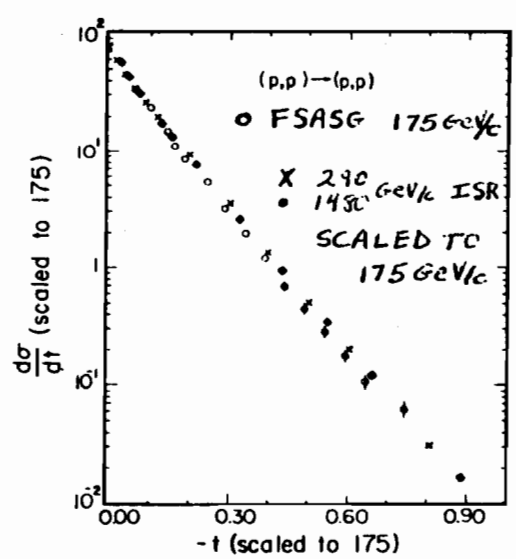

Fig. 10. Geometrical-scaling test for pp differential cross sections between 175 GeV/c and 290 and 1480 GeV/c. From Ref. 17.

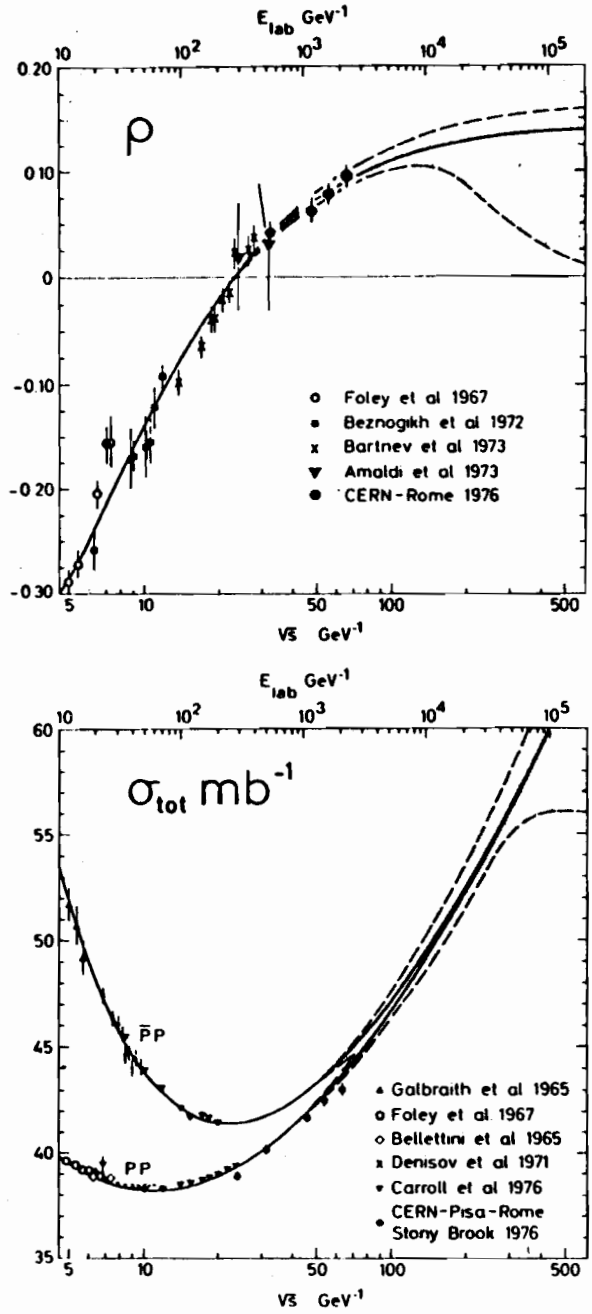

Fig. 11. From Ref. 28. Values of ρ and of total cross section for pp scattering up to $\sqrt{s}$ = 62 GeV. "The full curves are the result of a fit, simultaneously performed on the total cross section data and on the data for ρ" using dispersion relations.

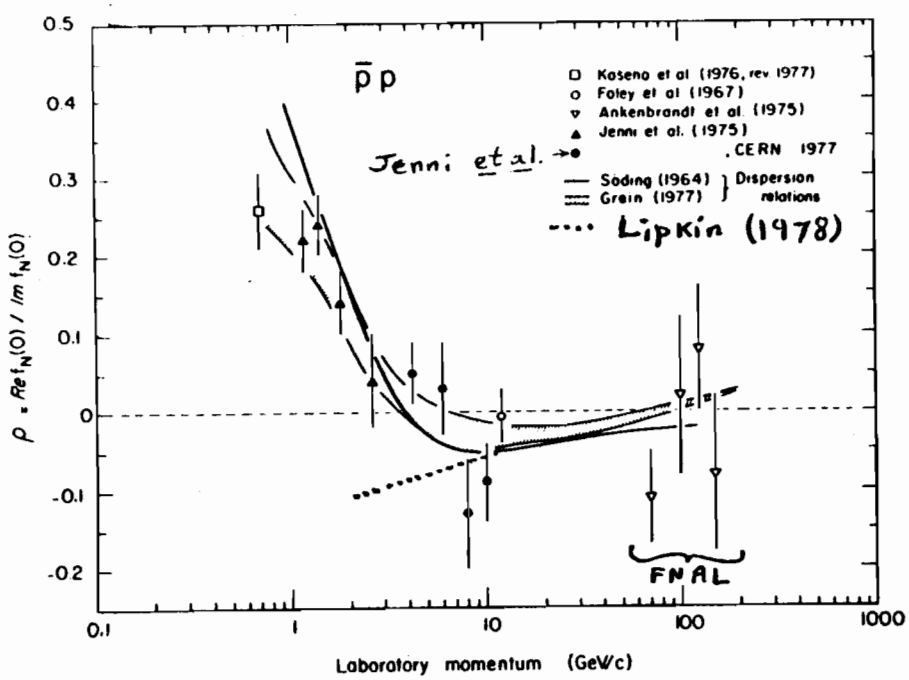

Fig. 12. Values of ρ for $\bar{p}p$ scattering up to 175 GeV/c laboratory momentum, from direct measurements using the Coulomb nuclear interference. From Ref. 30. Solid curves are the results of dispersion relation calculations. Dotted curve is a prediction of Lipkin, Ref. 7.

2.2 Real Part of the Forward Elastic Scattering Amplitude

If the rise in the total cross section is identified with the diffractive part of the scattering amplitude, then $\rho(s)$, the ratio of the real to the imaginary parts of the forward elastic scattering amplitude, must eventually become positive while decreasing as $(\ln s)^{-1}$. Dispersion relations connect $\rho(s)$ to total cross sections at much higher energy and provide a look ahead to these total cross sections as discussed by Hendrick and Lautrup[27]. The ratio ρ is given by the optical theorem,

$$1 + \rho^2 = 16\pi(d\sigma/dt)_{t=0}/\sigma^2_{tot}$$

Recent measurements have been reported by the CERN-Rome group[28] for pp scattering at very high energy, up to $\sqrt{s}$ = 62 GeV, exploiting the Coulomb-nuclear interference at very small t. As seen in Figure 11, ρ is found to be positive and still increasing, having crossed through zero at about 300 GeV/c. The authors conclude that the proton-proton (and presumably therefore, also the $\bar{p}p$) total cross sections should continue to increase at least up to an equivalent laboratory energy of 40 TeV, where they should reach a value of about 55 mb.

A recent measurement of ρ up to 400 GeV for pn scattering has been made by an Arizona-Dubna-Fermilab-Rochester group[29]. Similarily to the pp case, ρ_{pn} crosses from negative to positive at about 300 GeV/c.

Far fewer data exist yet for $\bar{p}p$ scattering, although considerably more data exist now than at the time of Reference 27. World data are shown in Figure 12, from a report of an experiment by a CERN group[30], and are compared with dispersion relation calculations of Soding and of Grein[31]. The theoretical curves of Hendrick and Lautrup[27] are very similar. No significant disagreement is apparent between theory and data, and in particular the data are consistent, within large errors, with the predicted 100 GeV/c crossover to positive values.

I have added to Figure 12 Lipkin's two-component Pomeron prediction[7] of the value of ρ, which is in reasonable agreement with the data from the highest measured point down to 8 GeV/c. Below that energy the agreement is very poor, probably reflecting the crudity of Lipkin's parameterization of the Reggeon exchange term(s). Lach[32] has

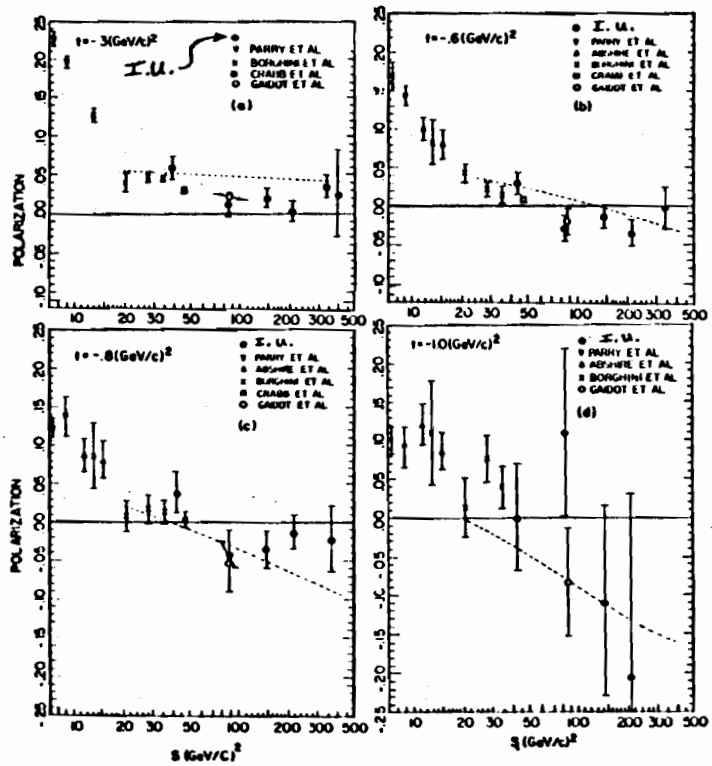

Fig. 13. Fron Ref. 32. Elastic p-p scattering polarization results at various fixed values of t. The curves are predictions of the model in Ref. 33.

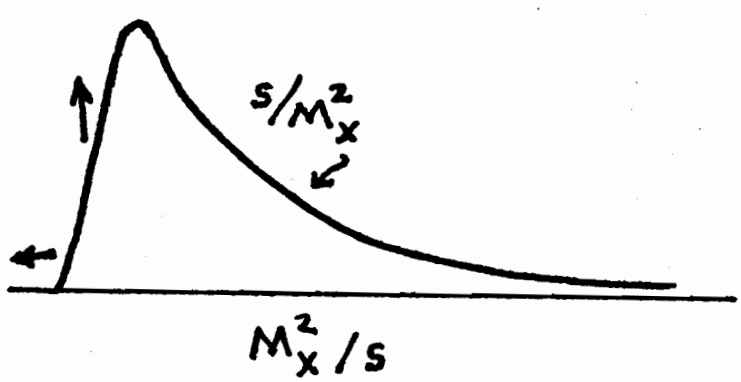

Fig. 14. Universal curve for the cross section of inelastic diffraction pp → pX as a function of the variable M_X^2/s, showing the s/M_X^2 dependence above the low mass peak, and indicating the region where the cross section is increasing as the kinematic boundary opens with increasing s.

reviewed the situation for $\rho(s)$ for all hadron beams, and conclude that agreement between data and dispersion relation predictions is reasonably good.

2.3 Elastic Polarizations

An Indiana University group[32] has measured the s and t dependence of the polarization of the recoil proton in pp elastic scattering at momenta between 20 and 200 GeV/c. The general features of the data, shown in Figure 13, are a decreasing value of the polarization with increasing s and negative values for large s when $-t \geq 0.6$ GeV^2. The data are consistent with a model of Pumplin and Kane[33], in which diffractive scattering with the exchange of two pions may become important at large s. This mechanism can cause a polarizations which persists to very high energy. The existing data, however, do not give strong support for non-zero polarizations at Fermilab energies.

3. Inelastic Diffraction

3.1 Single Diffractive Dissociation

The general features of very high energy inclusive diffractive dissociation of the proton

$$p + p \rightarrow p + X$$

are seen in a study at the ISR by the CERN-Holland-Lancaster-Manchester Collaboration (CHLM)[34]. The usual relatively low mass peak is seen in the mass of the system X recoiling against the proton. On the high mass side of the peak there is approximate $1/M_X^2$ dependence, which scales well in terms of the variable M_X^2/s. The peak of the M_X^2/s distribution moves down as s increases, following the kinematic boundary. This is shown schematically in Figure 14.

The measured cross sections integrated up to small fixed values of M^2/s rise by $\sim$ 15% to 35% as s ranges from 549 to 1464 GeV^2, with most of the rise concentrated at the lowest value of M_X^2 where the kinematic boundary is opening up. The inclusive differential cross sections (Figure 15) have steep t dependences which flatten out at large t, and are fitted by:

$$\frac{s}{\pi} \frac{d^2\sigma}{dM_X^2 dt} = A \exp(bt + ct^2)$$

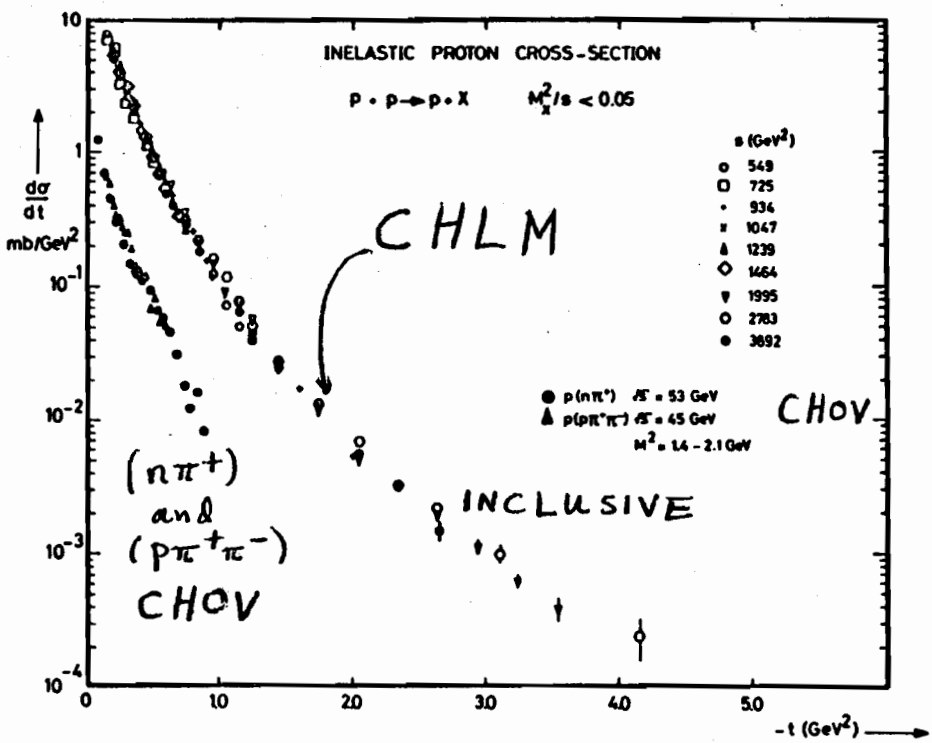

Fig. 15. From Ref. 34. The t-dependence of the inelastic pp cross section, integrated up to $M^2/s = 0.05$. Some data on exlcusive final states are also plotted.

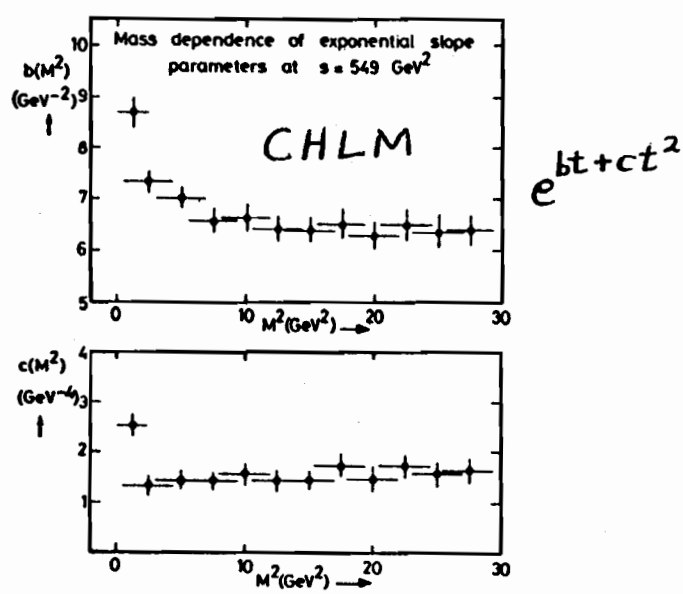

Fig. 16. From Ref. 34. Variation of the exponential slope parameters b and c as a function of M^2, for $\sqrt{s}$ = 549 GeV^2.

The parameters $b(M_x^2)$ and $c(M_x^2)$ are shown in Figure 16. For $M^2/s \gtrsim 0.01$ b is constant at ~ 6.5 GeV^{-2} and for lower M^2/s, b rises close to the elastic value of ~ 10 GeV^{-2}. At $-t > 1$ GeV^2 power law behavior begins to set in:

$$d\sigma/dt \sim s^{-m} f(\theta) \text{ with } m = 3.85$$

Such power law behavior has been derived for large angles, θ, where quark counting rules are obtained in parton and constituent interchange models[35]. The power law dependence seems to apply here at angles below 5°.

The cross section up to $M^2/s = 0.05$ or 0.10 for single diffractive dissociation (DD) of either beam or target proton varies from ~ 6 or 7 mb up to ~ 7 or 8 mb over the range of s studied (Figure 17). Lower energy Fermilab bubble chamber data and counter data are also shown, and have $\sigma^{DD} \sim 6$ to 7 mb. Diffractive dissociation of high energy protons on hydrogen and deuterium has been studied up to 372 GeV/c by a Fermilab-Dubna-Rockefeller-Arizona-Rochester group[36], who find a dominant $1/M_x^2$ behavior for $M_x^2/s \lesssim 0.05$, where also Pomeron factorization is found to hold.

Semi-exclusive diffraction, that is into a final state $N\pi$ or $N\pi\pi$, has been studied by a Saclay-Ecole Polytechnique-Rutherford collaboration[37]. They compare data from a 14.3 GeV/c K^-p bubble chamber experiment with pp data from the ISR and find that the shapes of the mass spectra, but not of the M^2/s spectra, are approximately independent of s, both in resonant and non-resonant diffractive dissociation components. This is in contrast to the inclusive high mass diffractive behavior found by CHLM. The semi-inclusive cross sections exhibit approximate vertex factorization properties.

3.2 Double Diffractive Dissociation

Double dissociation is difficult to study inclusively since neither target nor beam leads to a single final state particle which could be readily measured. Quite high energies are needed in any case to overcome substantial suppression by the kinematic limitations on the minimum momentum transfer, $-t_{MIN} = (M_c^2 - M_a^2)(M_d^2 - M_b^2)/s$, for the reaction $a + b \rightarrow c + d$.

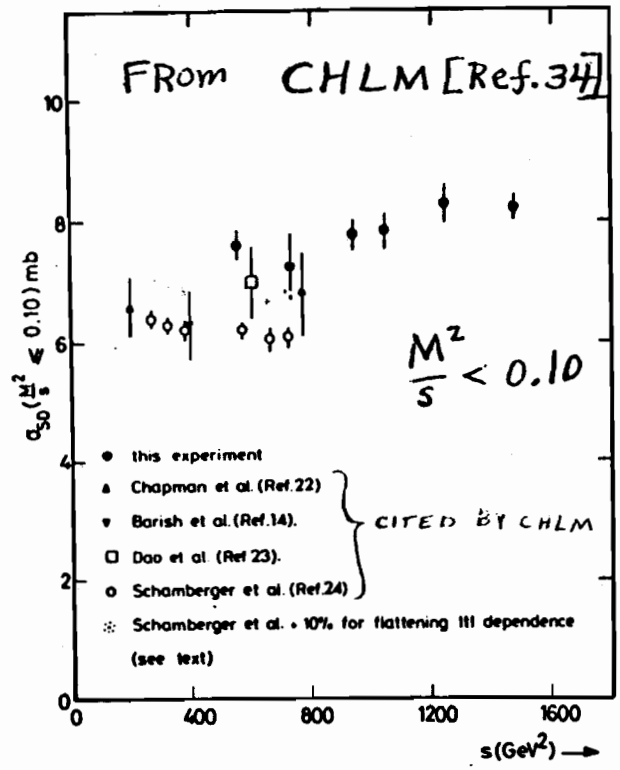

Fig. 17. From Ref. 34. Single diffractive cross section for $M^2/s \leq 0.10$, plotted as a function of M^2, for $\sqrt{s}$ = 549 GeV^2.

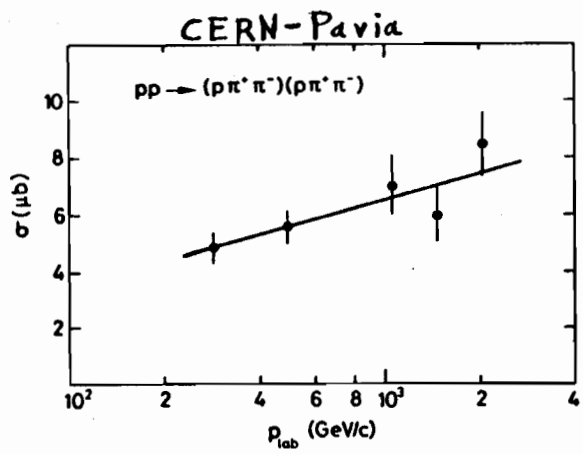

Fig. 18. From Ref. 38. Total cross section of $pp \to (p\pi^+\pi^-)(p\pi^+\pi^-)$ as a function of equivalent laboratory momentum. The line is a ln(s) fit to the data.

ISR measurements at the SFM have been made by the CERN-Pavia group[38] for the exclusive reaction $pp \rightarrow (p\pi^+\pi^-)(p\pi^+\pi^-)$. The cross section is shown in Figure 18, and is seen to increase by 55% as s goes from 549 to 3892 GeV^2. The cross section rise follows the form $A + B\ln(s)$. This rise, which is similar to the rise for low-mass ($M^2/s < 0.05$) inclusive single diffraction, again suggests an opening out of the kinematic boundary to lower masses as s increases.

The exponential t slope, b, in the expression $d\sigma/dt = Ae^{bt}$ shows a very strong dependence on the mass, M_X, of the diffractive system.[39] In Figure 19 one sees that b is quite large, greater than for elastic scattering, at the lowest value of M_X, and falls rapidly to an approximately constant value $\sim 2\ GeV^{-2}$ for M_X above 1.6 GeV/c^2.

This same group has studied the reaction $nn \rightarrow (p\pi^-)(p\pi^-)$ at $\sqrt{s} = 26$ GeV, again at the ISR/SFM[40]. The cross section of 11.5 ± 2.8 μb is comparable to the 5 μb cross section found for double dissociation of the proton into $p\pi^+\pi^-$, discussed previously. The mass of the excited $p\pi^-$ system is concentrated at quite low values, less than 1.8 GeV/c^2. An interesting dip in the differential cross section exists at $-t \sim 0.4$ GeV^2 and is particularly pronounced for the lowest diffractive masses. The forward t slope is again seen to be a steep function of M_X. The values observed of slope and cross section are consistent with the prediction of factorization, in which the dissociating particle at one vertex appears to be independent of the nature of the other vertex, that is, independent of whether the other vertex is a dissociation process or an "elastic" process. Figure 20 shows schematically how this factorization goes for simple Pomeron exchange. The simple factorization ratios must be modified by t_{min} effects for the double dissociation process.

3.3 General Features of Diffraction, and Relation to Elastic, Total and Inclusive Processes

Elastic, and single and double diffractive dissociation processes all have rather steep t slopes which, as well as cross sections, are related via vertex factorization. In addition, these processes share with total and inclusive processes the property of having cross sections which do not fall as s increase at large s. All these processes are

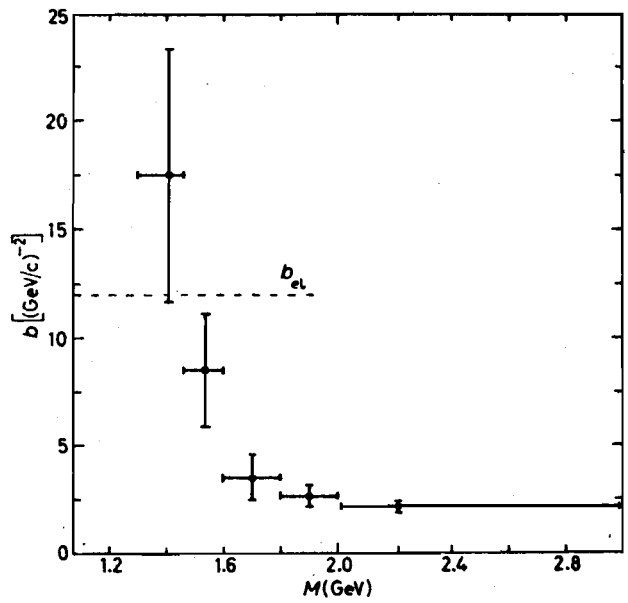

Fig. 19. From Ref. 39. Mass dependence of the exponential slope at $\sqrt{s}$ = 31 GeV, for the reaction pp → $(p\pi^+\pi^-)(p\pi^+\pi^-)$ for both diffractive masses within the given mass intervals.

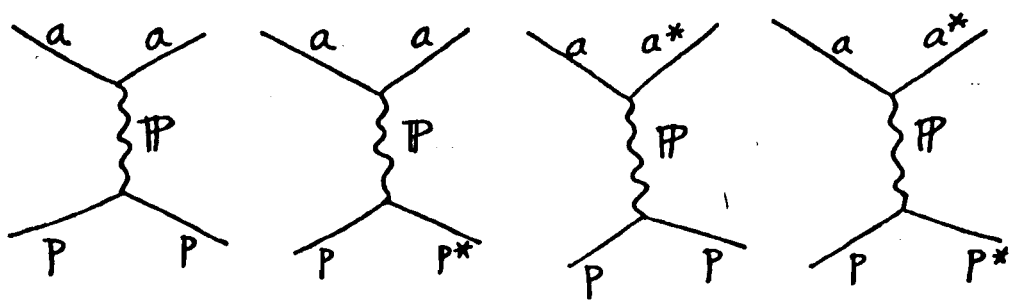

Amplitude $\sim g_{aa}g_{pp}$ $\quad g_{aa}g_{pp^*}$ $\quad g_{aa^*}g_{pp}$ $\quad g_{aa^*}g_{pp^*}$

Fig. 20. Pomeron exchange diagrams for elastic, single diffractive, and double diffractive scattering of hadron = a on a proton. Asterisk denotes diffractively excited system. Factorization hypothesis has the scattering amplitude proportional to the product of two factors, arising from the coupling at each vertex.

related through unitarity, and have been discussed by a number of authors in terms of a bare Pomeron intercept greater than one[41]. Experimental data on inclusive processes will be discussed in a following section.

Miettinen and Pumplin discuss total, elastic and inelastic diffractive processes in terms of the parton structure of hadrons[42]. They argue that all these "soft" diffractive processes involve the "wee" partons in each hadron, which will suffer variable interaction or absorption at each impact parameter, b. Moreover, since the absorption probability at each b necessarily lies between 0 and 1, one obtains the Pumplin bound[43]:

$$\sigma_{el}(b) + \sigma^{D}_{inel}(b) \lesssim \tfrac{1}{2}\,\sigma_{tot}(b), \text{ at each b}$$

At Fermilab and ISR energies, for pp scattering the data are:

$$7\text{mb} + (\lesssim 8\text{mb}) \leq 19.5\text{mb}$$

thus almost saturating the bound, and implying a very large spread in interaction probabilities of the wee partons. A novel and successful feature of the model is to consider fluctuations not only in rapidity and in impact parameter, but also in the number of partons. These three classes of fluctuation contribute to the diffractive cross section respectively 10%, 45%, and 45%. More importantily, it is the parton number fluctuations which contribute to the small t part of the differential cross section, and fill in the forward dip which appears as a failing of valence quark models of diffraction.

The authors use the magnitudes of the total and elastic scattering as input parameters, and derive the differential cross sections of both elastic and diffractive inelastic scattering, finding slopes of $\sim 11\ \text{GeV}^{-2}$ and $\sim 6\ \text{GeV}^{-2}$ respectively. They also obtain a cross section of $\sim$ 3mb for diffractive dissociation of beam (<u>or</u> target). Despite these successes, the model does not for the moment address the M_X^2 spectrum or the question of correlations between M_X and the exponential t slope.

The authors compare their model to the "active glue" model of Van Hove and Fialkowski[44], which is similar except that it has strong long range correlations.

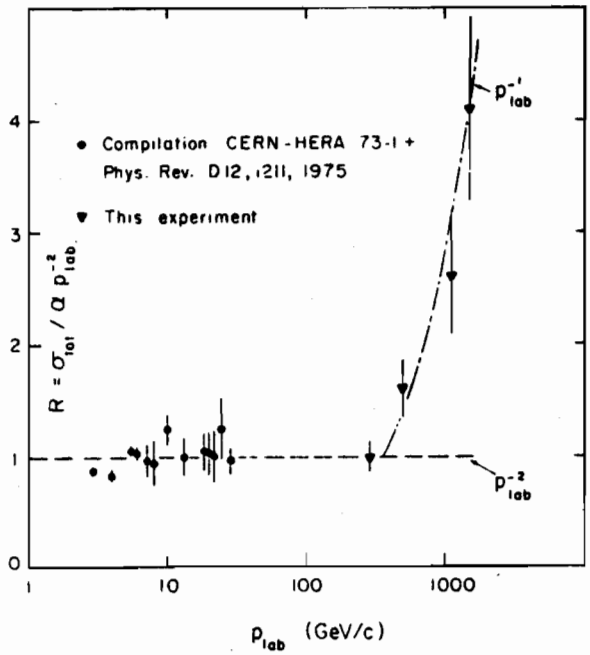

Fig. 21. From Ref. 45. "Total cross section of the reaction $pp \to n\,\Delta^{++}(1232)$ multiplied by the square of the equivalent laboratory momentum, as a function of p_{lab}."

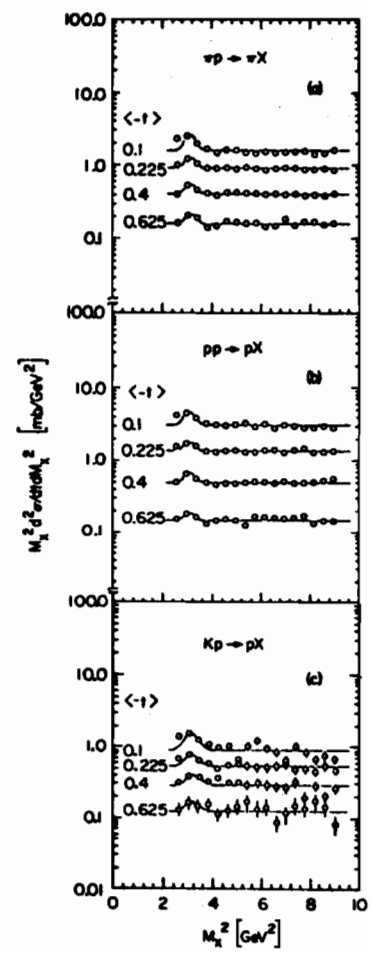

Fig. 22. From Ref. 49 part c. The invariant cross section $M_X^2 d^2\sigma/dtdM_X^2$ plotted vs. M_X^2 for (a) $\pi^+p \to pX$, (b) $pp \to pX$ (c) $K^+p \to pX$. Data at 140 and 175 GeV have been combined.

4. Charge Exchange Reactions

The reactions:

$$p\ p \rightarrow n\ \Delta^{++}$$

and

$$p\ p \rightarrow (p\pi^+)(p\pi^-)$$

have been measured respectively by the CERN-Hamburg-Heidelberg-Annecy-Vienna group (CHHAV)[45] and by CERN-Pavia[46] at the ISR/SFM from $\sqrt{s}$ = 23 to 53 or 63 GeV. The total cross sections, differential cross sections and decay angular distributions all indicate that ρ and A_2 exchange take over from π exchange at an equivalent laboratory momentum around 300 GeV/c. Figure 21 shows the abrupt transition from $\sim p_{LAB}^{-2}$ to $\sim p_{LAB}^{-1}$ behavior, corresponding to $\alpha_\pi(0) \sim 0$ and $\alpha_\rho(0) \sim \frac{1}{2}$.

Bouquet and Diu[47] and Diu and Ferraz de Carmargo[48] argue that both reactions have complicated exchange amplitudes and require an I = 1 exchange with large intercept, $\alpha(0) \sim 1$, to fit the abrupt change in p_{LAB} dependence of the cross sections.

The charge exchange reaction $\bar{p}p \rightarrow \Delta^{++}\bar{\Delta}^{--}$ has been studied up to 50 GeV/c, and is discussed more fully in section 6.

5. Inclusive Reactions

The Fermialb Single Arm Spectrometer has been used to measure inclusive hadron scattering

$$a + p \rightarrow a + X$$

where a is $\pi^\pm$, $K^\pm$ or $p^\pm$, at a series of momenta from 50 to 175 GeV/c, over a range $0.03 \leq -t \leq 0.7$ (GeV/c)^2 and Feynman x in the range $0.7 \leq x \leq 1.0$ up to the elastic peak[49]. In this region the triple Regge formalism is expected to apply with contributions by both Reggeon and Pomeron exchanges. In an earlier paper, the differential cross section $d^2\sigma/dtdM_x^2$ was found to vary as $1/M_x^2$ for a variety of values of t and for several beam particles (Figure 22). For the six beam types the invariant cross section s $d^2\sigma/dtdM_x^2$ factorizes approximately into a function of x times a function of t, as seen in Figure 23 where the x dependence is plotted for a series of ranges of t. This result can be reproduced by the triple Regge formalism. However, a much simpler empirical expression is used by the authors to fit the data, with two terms representing the Reggeon and Pomeron exchanges respectively.

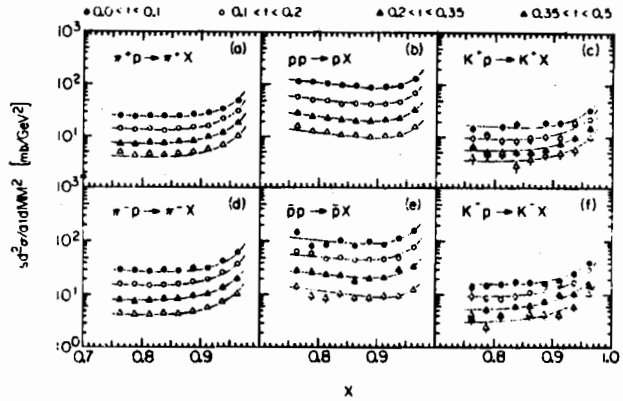

Fig. 23. From Ref. 49. Inclusive cross sections at 70 GeV/c for the six types of beam particles and for a variety of t intervals. The curves are fits to the forms given in the text.

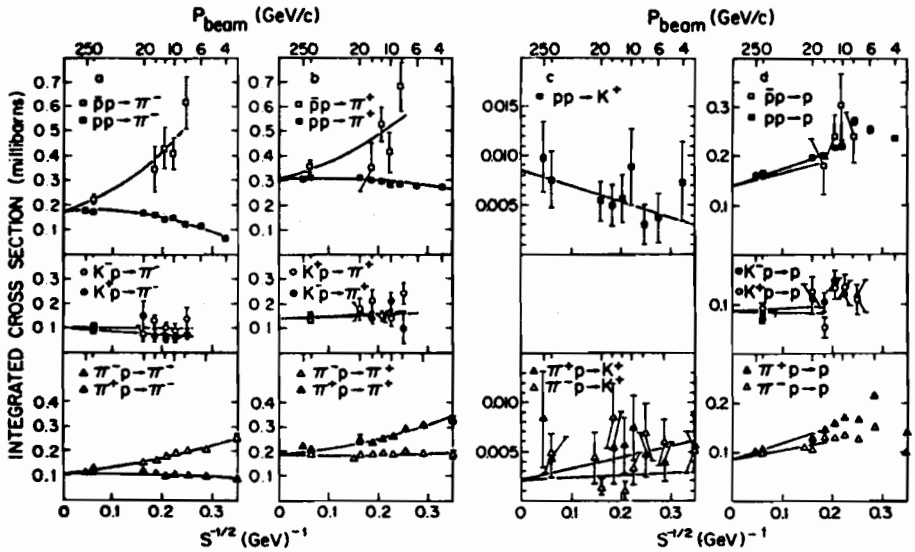

Fig. 24. From Ref. 50. Cross sections integrated over a certain portion of the proton fragmentation region, for the production of (a) π^- (b) π^+ (c) K^+ and (d) p, by all six types of incident charged hadrons on protons. Solid lines are fits to $A + Bs^{-\frac{1}{2}}$ or $A + Bs^{-\frac{1}{2}} + Cs^{-1}$.

$$s\, d^2\sigma/dtdM_x^2 = A_1(s,t)(1 - x) + A_2(s,t)/(1 - x)$$

where $$x \approx 1 - (M_x^2 - M_p^2)/s$$

and $$A_i = A\exp(Bt + Ct^2)(1 + D(E^{-\frac{1}{2}} - 0.1))$$

The Pomeron term, A_2, is reasonably well represented by a simple exponential, $C \ll B$. The Reggeon term has $C \approx B$ and exhibits a strong change of slope. The diffractive (Pomeron) term exhibits significant energy dependence, not expected for a triple Pomeron process. Away from $x \approx 1$ all particles show little energy dependence.

Factorization in a model where a single Reggeon trajectory dominates both the elastic and inelastic cross sections would imply that, near $x = 1$, the ratio $d\sigma_{inelastic}(t)/d\sigma_{el.}(t)$ should be independent of the beam particle. It is found that as x decreases the p and $\bar{p}$ cross sections increase relative to the π and K cross sections (Figure 23) and consequently A_1/A_2 is ~ 100 for $p^{\pm}$ while for mesons it is ~ 50. This severe departure from factorization may be accounted for by an extra $\pi\pi P$ term which is allowed only for $p^{\pm}$, or alternatively the effect may be due to decay products from the diffractive nucleon peak. The corresponding decay products from diffractive dissociation of meson beams will tend to appear at lower x due to the more nearly equal masses of the decay products.

A University of Pennsylvania group has measured the inclusive cross sections

$$a + p \rightarrow c + X$$

from 4 to 250 GeV/c at BNL and FNAL, where particles a and c are $\pi^{\pm}$, $K^{\pm}$, or $p^{\pm}$ and are not necessarily the same[50]. The data are taken in a small fixed portion of the proton fragmentation region with $p_T = 0.3$ GeV/c and laboratory rapidity $y_L = 0.6$, 0.4, and 0.2 for produced π, K, and p respectively. The authors also list several earlier bubble chamber studies of inclusive particle production which cover a wider range of phase space but which have limited statistics and in general do not identify the final state particles as kaon, pion, or proton.

The energy dependence $A + B\, s^{-\frac{1}{2}}$ of the differential cross sections predicted by Mueller-Regge phenomenology is tested in Figure 24, and it is found that the low energy part of the data requires a further

term, $A + B\, s^{-\frac{1}{2}} + C\, s^{-1}$, in the case of produced pions, particularly when the incident beam is $p^{\pm}$. Good fits are obtained under the assumption that A, the high energy asymptotic value of the differential cross section, is the same for incident particle and antiparticle. In the high energy region the particle-antiparticle cross section differences are seen to vary as $s^{-\frac{1}{2}}$; and to vanish in agreement with the strong prediction of Pomeron factorization that:

$$\frac{E\, d^3\sigma/d^3p\ (ap \to c)}{E\, d^3\sigma/d^3p\ (a'p \to c)} = \frac{\sigma_{tot}\ \ (ap)}{\sigma_{tot}\ (a'p)} \qquad s \to \infty$$

Further tests of this relation obtained by comparing meson beams and proton beams are shown in the following table. The total cross sections are taken from fits of Hendrick et al.[6] evaluated at 250 GeV/c.

	Asymptotic Measured Cross Section				Total Cross Section Ratio
	$c = \pi^-$	$c = \pi^+$	$c = K^+$	$c = p$	
$\frac{(\pi p \to c)}{(pp \to c)}$	0.63 ± 0.03	0.62 ± 0.03	0.25 ± 0.18	0.62 ± 0.03	0.61 ± 0.02
$\frac{(Kp \to c)}{(pp \to c)}$	0.60 ± 0.06	0.45 ± 0.04		0.61 ± 0.08	0.53 ± 0.02

The agreement is reasonably good, with the exception of the point for produced K^+, which has large experimental errors.

6. Exclusive Final States

In two papers submitted to this conference, the Amsterdam group treat four-prong $\bar{p}p$ events at 7.2 GeV/c, and give cross sections for a variety of 4-constraint and multiple-missing-neutrals final states. In the four-constraint channel they separate diffractive dissociation and the final state $\Delta^{++}\bar{\Delta}^{--}$, and give energy dependences. In a recent paper[51] this group discuss $\bar{p}p \to \bar{p}pM^o$ and other exclusive channels, where M^o is some neutral meson, and give cross sections for:

$M^o =$	ρ^o	ω	φ	η	η'
σ (μb)	115 ± 35	228 ± 13	4^{+5}_{-2}	56 ± 14	18 ± 6

The measured ratio of φ to ω cross sections implies that the vector meson nonet mixing angle differs from the ideal mixing angle ($\tan^{-1}\sqrt{\frac{1}{2}}$) by $= (9^{+3}_{-7})^o$ and is therefore compatible with a value $\theta_{1^-} = (44^{+7}_{-3})^o$, to be compared with the value of 40° calculated using the Gell-Mann Okubo mass formula. The OZI rule suppresses production of $s\bar{s}$ pairs and hence production of the φ; however, nonet mixing can account for the observed

amount of φ and no OZI violation is needed.

Comparing with data at other energies the authors find $\left|A_{\bar{p}\omega p}\right|^2 \sim s^{-2.7 \pm 0.3}$. However, the amplitude A is given by $A^2 = \sigma/R$ where R involves phase space and flux factors and accounts for some 2 units of the exponent of s, with $\sim$ 1 unit coming from the variation of the cross section. This result can be compared with the treatment by the Liverpool-Stockholm group (L-S)[52] with 9.1 GeV/c $\bar{p}p$ data, who find $\sigma \sim s^{-0.9} = s^{2\alpha(0)-2}$ implying an intercept $\alpha(0) \sim 0.5$, and hence that the double Pomeron process is not yet important as these energies.

The Liverpool-Stockholm group also report observation of $N^*(1800) \to p\omega$, $\bar{p}\omega$ with a width of 145 ± 70 MeV/c^2 and a cross section of 25 ± 5 μb, to be compared with 28 ± 6 μb at 5.7 GeV/c (CERN-Prague[53]). The authors conclude that this N* is probably diffractively produced, and by the Gribov-Morrison rule $\Delta P = (-1)^{\Delta J}$, it probably has $J^P = \frac{1}{2}^+$ or $3/2^-$. In an earlier paper, L-S[54] report various exclusive and inclusive cross sections for production fo Δ^{++}, ρ^o, and ω in non-annihilation and annihilation reactions.

For the reaction $\bar{p}p \to \bar{p}p\pi^+\pi^-$ I report preliminary 50 GeV Purdue data, which are also compared with lower energy data, including the recently published 32 GeV/c data[55]. Reports submitted to this conference on this final state include the above mentioned 7.2 GeV/c Amsterdam data, 22.4 GeV/c data by the Alma Ata-Dubna-Helsinki-Moscow-Prague collaboration, 32 GeV/c data (France-Soviet Union and CERN-Soviet Union collaboration) and remarks on pion exchange in this reaction, by Wolters.

At 50 GeV some 306 events fit this 4-C hypothesis, for a cross section of 1.23 ± 0.07 mb; and only one event makes a questionable fit to the hypothesis $pp \to \pi^+\pi^-\pi^+\pi^-$, corresponding to a cross section less than 0.016 mb at 90% confidence level. The energy dependences of the two reaction cross sections are plotted in Figures 25 and 26 where the very low cross section for the annihilation reaction is consistent with the roughly $s^{-2.8}$ dependence observed at lower energies. The cross sections for the non-annihilation reaction at 32 and 50 GeV are compatible with the extrapolated $s^{-0.47 \pm 0.04}$ energy dependence observed between 3.5 and 12 GeV/c[55]. At the higher energies this reaction is dominated by

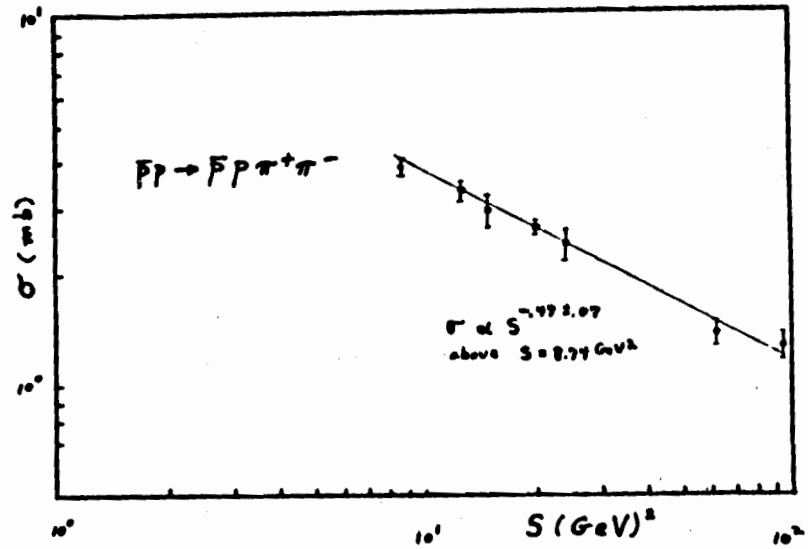

Fig. 25. World data for the reaction $\bar{p}p \to \bar{p}p\pi^+\pi^-$, cross section vs. s. The power law fit to the lower energy data is from Ref. 57.

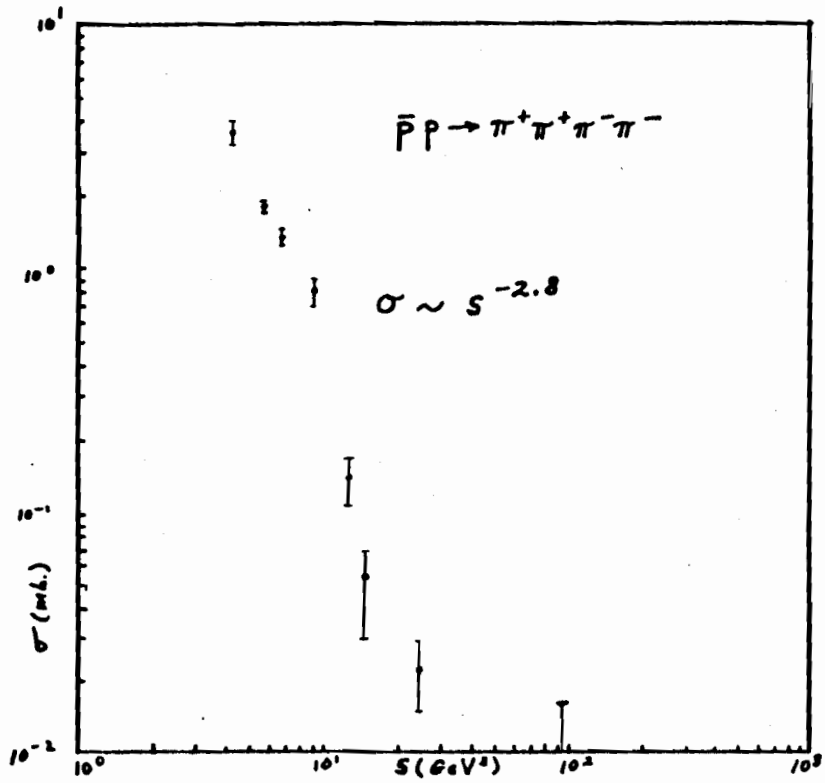

Fig. 26. World data for the reaction $\bar{p}p \to \pi^+\pi^+\pi^-\pi^-$, cross section vs. s. The point at p_{lab} = 50 GeV/c is an upper limit. The aproximate power law dependence is based on a hand drawn line through the lower energy points.

beam and target diffraction into ($p^{\pm}\pi^{+}\pi^{-}$), as seen in Figure 27 for 50 GeV/c. The low-mass diffractive enhancement extends up to about 2.7 GeV/c^2, and consists mostly of $\Delta\pi$. Events containing a Δ^{++}or $\bar{\Delta}^{--}$ (defined as $M(p^{\pm}\pi^{\pm}) < 1.4$ GeV/c^2) are shaded and constitute almost all of the events below $M(N\pi\pi) = 2$ GeV/c^2. The cross section for beam diffraction into $\bar{p}\pi^{+}\pi^{-}$ is tabulated below for the 32 and 50 GeV/c data and for the CERN-IHEP boson spectrometer data at 25 and 40 GeV/c[56]. The diffractive enhancement extends to progressively higher masses with increasing s, and the diffractive cross section so defined in this exclusive channel is seen to rise with energy, and to become an increasing fraction of the total final state.

Pinc (GeV/c)	25	32	40	50
$\sigma^{DD}_{\bar{p}}\to p\pi^{+}\pi^{-}$(mb)	0.30 ± .01	0.38 ± .04	0.34 ± .02	0.45 ± .04
cuts	M < 2.2	M < 2.5	M < 2.6	M < 2.7
$\frac{\sigma^{DD}_{\text{Beam or target}}}{\sigma_{pp\pi^{+}\pi^{-}}}$		0.57 ± .06		0.73 ± .07

Other features of the diffractive channel observed by the CERN-IHEP spectrometer are: exponential fall-off with increasing t, with shallower t-slopes as $M(N\pi\pi)$ increases; below 1.5 GeV/c^2 the system has $J^P = \frac{1}{2}^+$; above 1.5 GeV/c^2 there is at least one state of $J \geq 3/2$ and there is interference between states of opposite parity; and a state of $J \geq 5/2$ is present in the region 1.7 to 1.8 GeV/c^2.

While falling fairly rapidly, some $\Delta^{++}\bar{\Delta}^{--}$ persists at higher energies, and the cross section at 50 GeV/c is measured to be 0.07 ± 0.02 mb. The dependence of this cross section on energy is plotted in Figure 28, and varies approximately as $s^{-1.33}$ with a good overall fit to simple power law dependence up to 50 GeV/c, corresponding to a Regge intercept $\alpha(0) \sim 0.34$. The L-S group[57] fit an exponent -1.39 ± .11 at lower energies, and find in their 9.1 GeV/c data evidence for exchange of more than one Regge trajectory, namely a break in the slope of the differential cross section, and non-zero values of certain combinations of the joint statistical decay tensors.

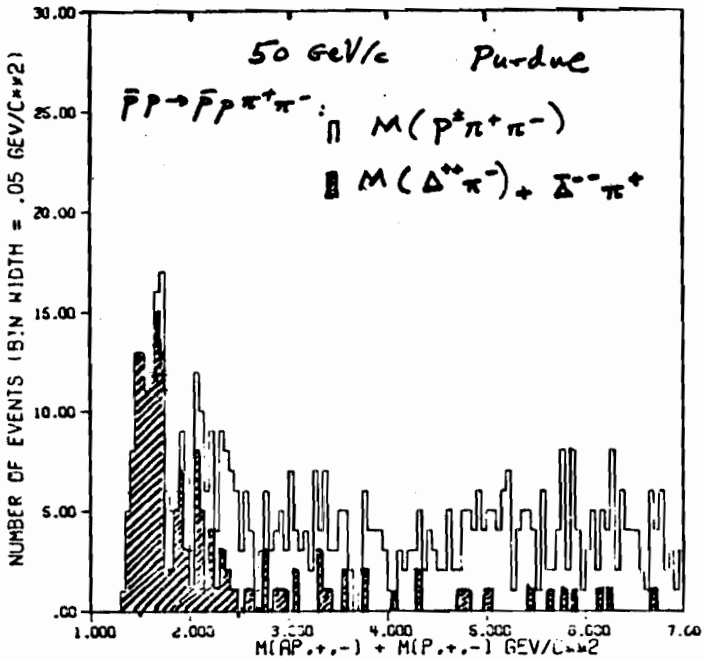

Fig. 27. Purdue 50 GeV/c data, $\bar{p}p \to \bar{p}p\pi^+\pi^-$: Mass of $(p^\pm\pi^+\pi^-)$ system. Shaded events are $\Delta^{++}\pi^-$ or $\bar{\Delta}^{--}\pi^+$, where Δ is defined as $M(N\pi) \leq 1.4$ GeV/c^2.

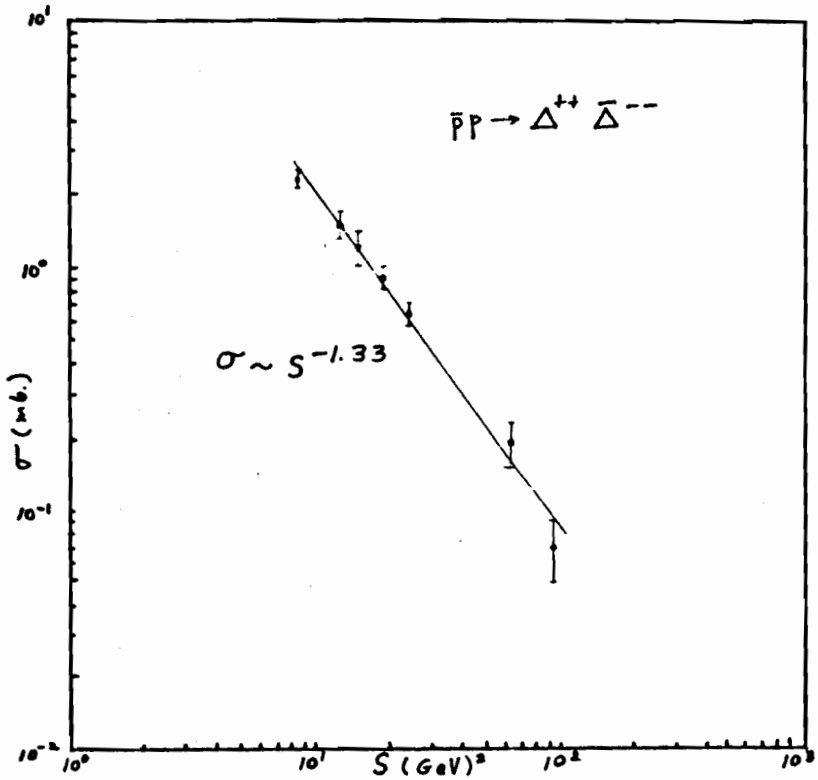

Fig. 28. World data for the reaction $\bar{p}p \to \Delta^{++}\bar{\Delta}^{--}$, cross section vs. s. The power law dependence is based on a hand fit to all data points.

Exclusive 4-C final states of charge multiplicity 6, 8, and 10 are reported for the 32 GeV/c data, and cross sections are given for both annihilation and non-annihilation reactions[55].

In an attempt to study double Pomeron exchange, a CERN-College de France-Heidelberg-Karlsruhe collaboration has studied the reaction $pp \rightarrow pp\pi^+\pi^-$ at $\sqrt{s}$ = 31 GeV,[76] in the split field magnet. After kinematic fitting and cuts to ensure leading protons and large rapidity gaps between the dipion system and either proton, a sample remains which corresponds to 25 ± 10 μb. The distribution in the sum of the squares of the transverse momenta of the two protons, $p_{T1}^2 + p_{T2}^2$, is exponential with a slope $B = (-5.5 \pm 0.9)(GeV/c)^{-2}$, as expected for double Pomeron exchange when compared to elastic scattering analyzed in terms of factorization. The two protons are uncorrelated in azimuth and in p_T. And the dipion system is isotopic and is consistent with a low-mass s-wave enhancement. The authors observe that while all this does not prove the presence of the double Pomeron exchange process, it is completely consistent with the predictions of the model.

7. Neutral and Strange Particle Production

Some recent results from antiproton-proton experiments include:

100 GeV/c	Cambridge-Fermilab-Michigan State (30" HBC)[58]
50 GeV/c	Purdue (new data)
32 GeV/c	France-Soviet Union and CERN-Soviet Union (Mirabelle)[55]
12 GeV/c	Brussels-CERN-Imperial College-Mons-Orsay (BEBC)[59]
3 GeV/c	Brandeis-Cincinnati-Syracuse (BNL-Multiparticle Spectrometer(MPS))[60]

This last experiment, as well as the following experiments, have reports submitted to this conference:

22.4 GeV/c	Alma Ata-Dubna-Helsinki-Moscow-Prague-Tbilisi (Ludmila HBC)
7.3 GeV/c	Amsterdam-Athens-Demokritos-Liverpool-Vienna (CERN 2m HBC)
4.1 GeV/c	Notre Dame-Tennessee-ORNL-ANL-Melbourne (12' HBC+ TST)
3.6 GeV/c	Tata Institute
0.76 GeV/c	Bombay-CERN-College de France-Madrid

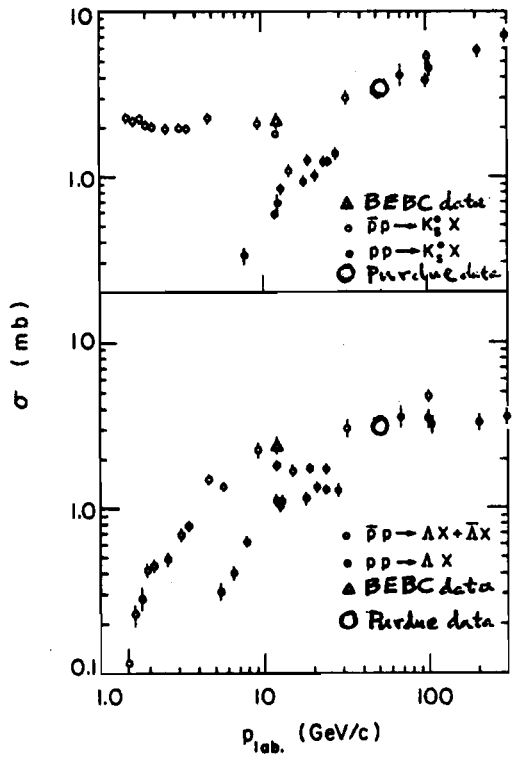

Fig. 29. From Ref. 59. "Inclusive cross sections for the reactions $\bar{p}p \rightarrow K^{o}_{s}$ X and $\bar{p}p \rightarrow \Lambda^{o}$ X + $\bar{\Lambda}^{o}$ X as a function of beam momentum. For comparison the cross sections for the reactions pp → K^{o}_{s}X and pp → Λ^{o}X are also shown." Purdue data points at 50 GeV/c have been added.

The MPS data correspond to 150 events/μb. $\bar{\Lambda}\Lambda$, $\bar{\Lambda}\Sigma^{o}$, $\bar{\Sigma}^{o}\Lambda$ and $\Lambda(1520)$ production are seen and cross sections are presented, but no $\Lambda(1405)$ or $\Sigma(1385)$ are observed. The distributions of $d\sigma/dt'$ and Λ polarization for the first two reactions are compatible with some proposed Regge exchange models[61].

The 12 GeV BEBC data are very numerous, with 6300 fitted K^{o}_{S} and 6300 fitted Λ or $\bar{\Lambda}$. Distributions in x_F, $y = \frac{1}{2}\ln[(E + P_{||})/(E - P_{||})]$, p_T, and charge multiplicity n_c are presented. The K^{o} are centrally produced and the Λ ($\bar{\Lambda}$) are mainly associated with target (beam) fragmentation. The average charge multiplicity, $< n_c >$ is studied as a function of M_x^2 for $pp \rightarrow V^{o}X$ where V^{o} is K^{o}_{S}, Λ or $\bar{\Lambda}$. The characteristic dependence $< n_c > \sim \ln(M_x^2/1\ \mathrm{GeV}^2)$ is observed as it is in a variety of single particle inclusive reactions[62]. For comparison the total $< n_c >$ for $K^{-}p$ interactions as a function of s is studied, since this system has the same quantum numbers (or the charge conjugate thereof) as the $X_{\Lambda,\bar{\Lambda}}$ system recoiling against $\Lambda,\bar{\Lambda}$. The agreement is striking.

By comparing with $pp \rightarrow K^{o}_{S}$ it is found that annihilations are important for K^{o} production, which is also associated (in $\bar{p}p$ but not in pp) with higher $< n_c >$ than is Λ production. A substantial sample of events with two neutral strange particles is studied for correlations. The K^{o}_{S} and $\Lambda + \bar{\Lambda}$ cross sections as a function of energy are shown for $\bar{p}p$ and pp interactions, in Figure 29 from this paper. I have added the 50 GeV points from Purdue data. The $\bar{p}p$ and pp inclusive K^{o} cross sections are approaching a common value, which increases with energy. For $\Lambda/\bar{\Lambda}$ production the cross section is relatively flat at high energy, and the production by $\bar{p}p$ remains above that by pp interactions.

100 GeV data are used to check Dao and Whitmore's[63] extension of Koba Nielson Oleson (KNO) scaling for π^{o} production:

$$\frac{< n > \sigma_n(\pi^{o})}{< n_{\pi^{o}} > \sigma_{incl}} = \varphi(n/< n >)$$

and an analogous relationship for K^{o}_{S} and Λ, by Cohen[64]. These are shown in Figure 30 and are compared with fits to pp data. The K^{o}_{S} data scale well, whereas the Λ data do not, although they do agree with the 100 GeV pp data suggesting that at 100 GeV and above scaling may hold. It is worth noting that $\bar{\Lambda}$ and Λ are produced from beam (target)

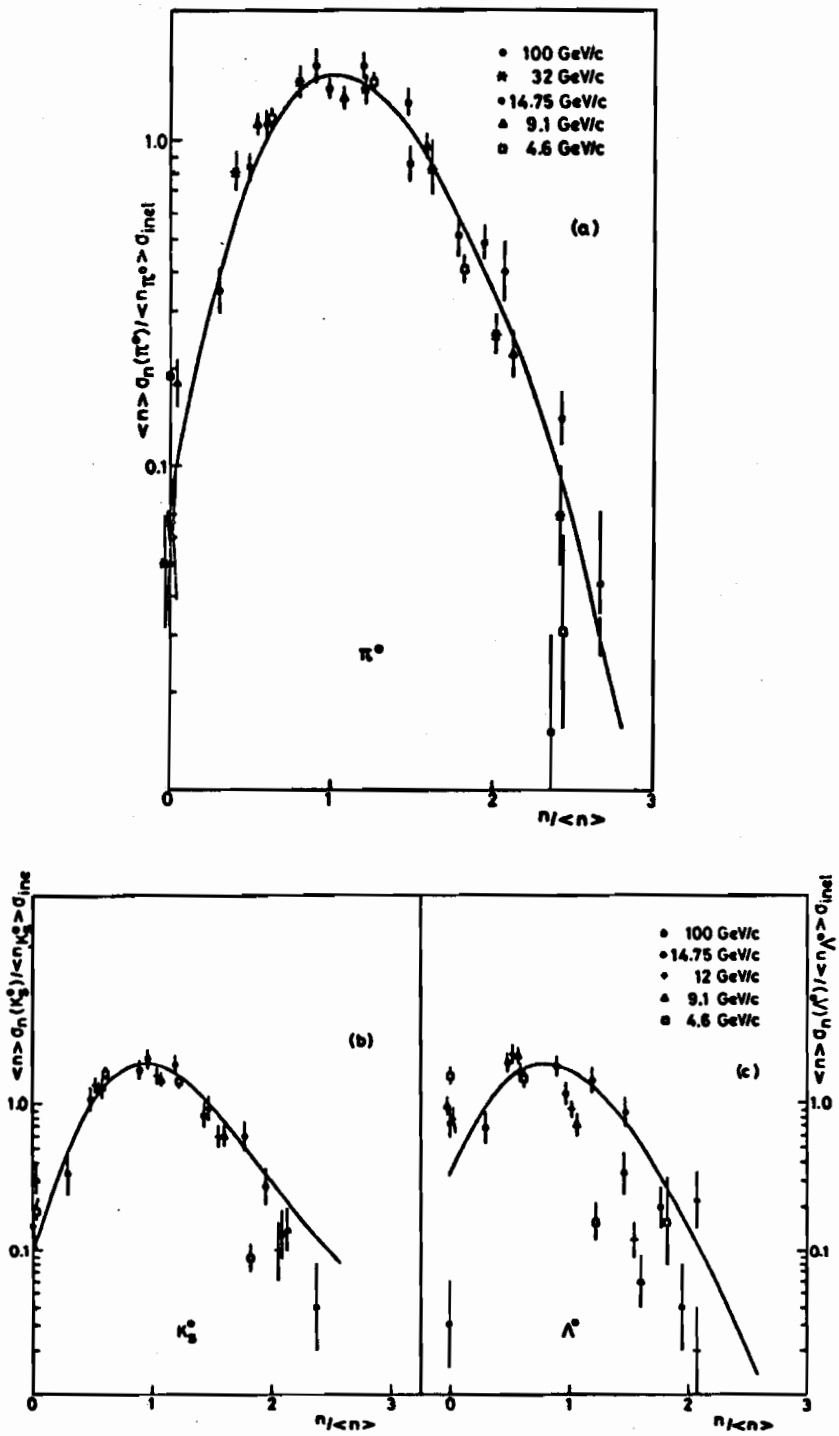

Fig. 30. From Ref. 58. Generalized scaling of neutral topological cross sections, $< n > \sigma_n(\pi^o)/< n_{\pi^o} > \sigma_{inel.}$ vs. $n/< n >$ for (a) $pp \rightarrow \pi^o$ (b) for K^o_s (c) for Λ^o. The curves are fits to high energy pp data.

fragmentation, perhaps diffractively, whereas the K^o and π^o are more centrally produced, and the two mechanisms may have quite different energy dependence.

Another kind of scaling is the Regge-Mueller prediction that central production of any particle type in $a^{\pm}$ scattering, where a^+ and a^- are particle and antiparticle, should approach a common asymptotic value as $s^{-\frac{1}{4}}$. Figure 31a-c, from Reference 58, shows the invariant structure functions $F_1(x)$ for γ, K^o_S, and Λ for 100 GeV/c $\bar{p}p$ and pp scattering and for 14.7 GeV/c $\bar{p}p$ scattering. I have added curves and points for the 12 GeV/c and 50 GeV/c data, respectively. The distributions are very similar except for: (a) the tendency for the K^o inclusive distributions to peak somewhat more sharply toward x = 0 at higher energies (b) anomalous behavior of the 14.7 GeV K^o data, which are therefore questionable (c) an excess of centrally produced $\Lambda/\bar{\Lambda}$ in $\bar{p}p$ compared to pp interactions (perhaps an annihilation effect).

Plotting the invariant structure function $F_1(x = 0)$ against $s^{-\frac{1}{4}}$ in Figure 31 d-f one finds that the Λ production data scale well in energy and are approximately equal for both $\bar{p}p$ and pp interactions. However, by CP symmetry an equal amount of $\bar{\Lambda}$ production takes place at x = 0 in $\bar{p}p$ interactions. Since $\bar{\Lambda}$ production is largely absent in pp interactions, the overall Λ plus $\bar{\Lambda}$ production is thus considerably larger in $\bar{p}p$ than in pp interactions. Central K^o and γ production are still increasing with energy, but in each case the $\bar{p}p$ - pp difference seems to be approaching zero, with the excess always attributable to the $\bar{p}p$ data and presumably due to annihilations. For $\bar{p}p$, $F_1^{\gamma}(0)$ has a minimum at an intermediate energy around 25 GeV, and rises rather steeply for energy increasing or decreasing. At high energy the data are consistent with the predicted $s^{-\frac{1}{4}}$ behavior over the range studied.

8. Vector and Tensor Meson Production

Papers submitted to this conference deal with the following resonances:

$K^*(890), \Sigma(1385)$	14.75 GeV/c	Tufts-Tohoku-Michigan State-FNAL
$\rho, \omega, f, K^*, A_2$	9.1 GeV/c	Liverpool-Stockholm
ρ, Δ^{++}	32 GeV/c	France-Soviet Union and CERN-Soviet Union

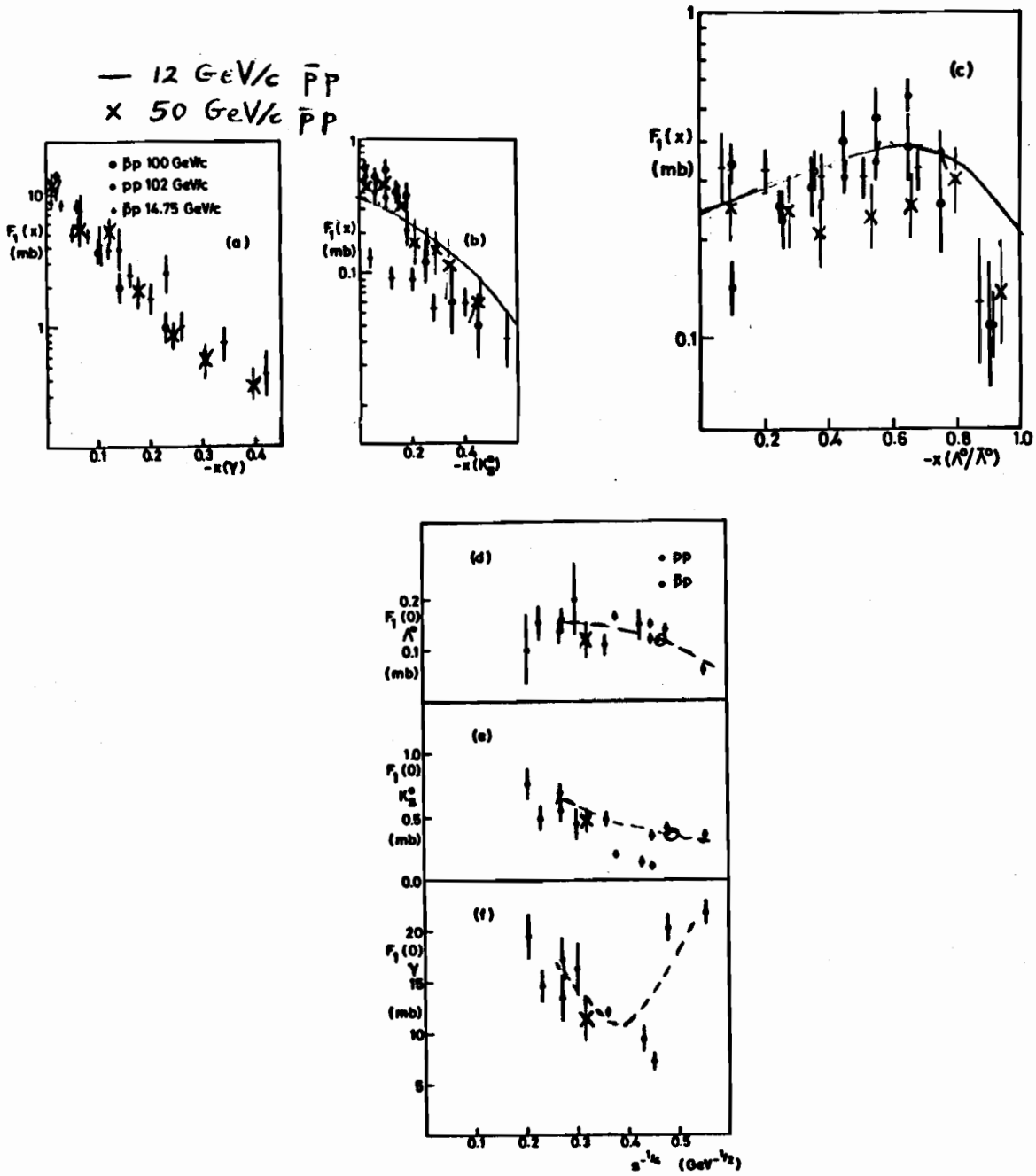

Fig. 31. From Ref. 58. The invariant cross section

$$F_1(x) = \int \frac{2E d^2\sigma}{\pi\, s\, dx dp_T^2}\, dp_T^2$$

vs x for (a) γ, (b) K_S^o, and (c) Λ^o, $\bar{\Lambda}^o$, for 102 GeV pp and for 100 GeV/c and 14.7 GeV/c $\bar{p}p$. Added are 12 GeV/c and 50 GeV/c $\bar{p}p$ curves and points. (d-f) $F_1(0)$ for pp and $\bar{p}p \to \Lambda^o$, K_S^o, and γ as a function of $s^{-\frac{1}{4}}$. 12 GeV/c $\bar{p}p$ data have been added, and the dashed curve is to guide the eye to the $\bar{p}p$ data.

In addition, I shall refer to the CFM 100 GeV/c $\bar{p}p$ studies of ρ^o and f^o production[65], and of K* production[68] and present new 50 GeV Purdue data on ρ^o production.

The L-S group find at 9.1 GeV/c an upper limit on $K^{*\pm}$ production of 0.17 and 0.33mb, respectively, for the sum of annihilations plus non-annihilation interactions, corresponding to $K^{*\pm}/K^o$, $\bar{K}^o \leq 0.14 \pm 0.1$. TTMF at 14.7 GeV/c find $\sigma(K^{*+})/\sigma(K^o) = 0.31 \pm 0.03$. The FNAL-Cambridge-MSU group find no K*(890) at 100 GeV/c, with a one standard deviation upper limit of 0.45 mb. The general conclusion if that at least a significant fraction of the neutral kaons do not come from vector meson production. A similar conclusion is reached in a study of 205 GeV pp interactions, by an ANL-Stony Brook-FNAL group[66] who find a 95% confidence level upper limit of $0.22K^{*\pm}$ per inelastic event, and a ratio $K^{*\pm}/K^o = 0.32^{+0.14}_{-0.18}$. As discussed in Ref. 66, this result is incompatible with the analysis reported by a recent ISR experiment at $\sqrt{s} = 53$ GeV[67], where the authors fit the correlated $\pi^+\pi^-$ mass distribution by an incoherent sum of ρ^o, ω^o, η^o, f^o, K^{*o}, with the charged kaons treated as pions since there was no final state mass identification in the experiment. There is no direct evidence for K*. This indirect procedure leads to very large estimates of the amount of K*, ρ^o, and ω^o, each greater than one per inelastic event. Among other consequences is a ratio $\rho^o/\pi^- = 0.25 \pm 0.05$ at $\sqrt{s} = 53$ GeV, a result twice as large as is found in most lower energy pp and $\bar{p}p$ experiments, to be discussed below.

The L-S group can account for some (36 ± 6)% of the non-annihilation π^- production from ρ^o, p^-, ω^o, f^o and Δ^{--} production, and conclude that a large fraction of pions cannot be accounted for by parent resonances. In particular they quote a ratio of $\rho^o/\pi^- = 0.07 \pm 0.02$ for non-annihilation reactions. They tabulate world data for pp, and $\bar{p}p$ non-annihilation, between 9 and 205 GeV, with the above ratio lying between 0.07 and 0.12. (For annihilations events, the ratio is found to lie between 0.13 and 0.18 over a wide energy range.) More recent data for $\bar{p}p$ (total) interactions at 32, 50, and 100 GeV/c are consistent with this general pattern: From the inclusive ρ^o cross section at 32 GeV/c, (9 ± 1.6)mb, and the published π^o cross section[68]

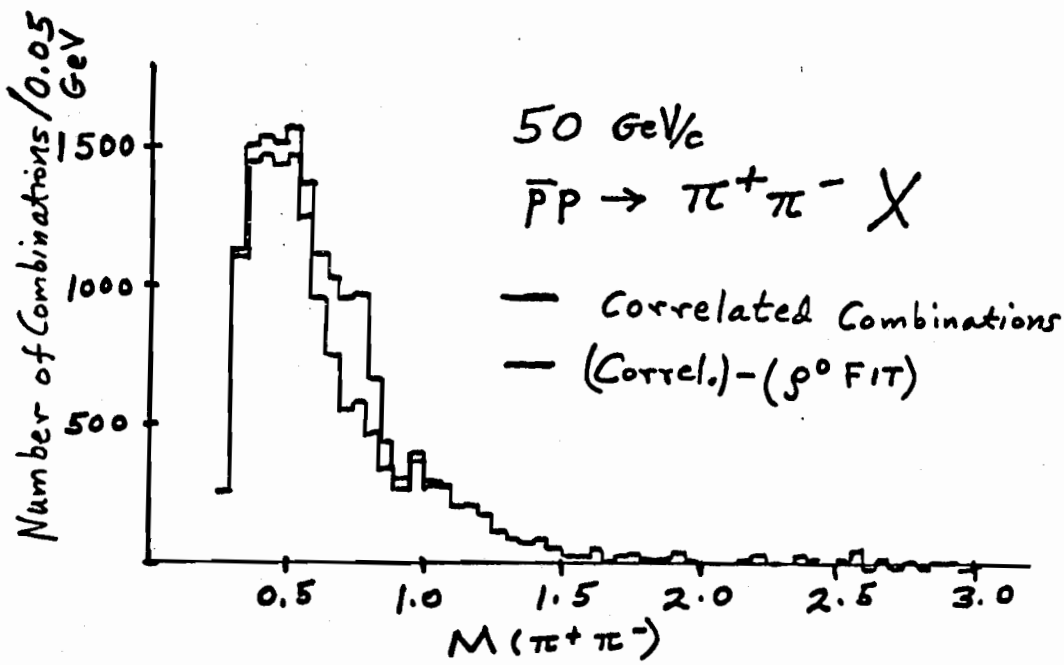

Fig. 32. Purdue 50 GeV/c $\bar{p}p$ data: Inclusive correlated $\pi^+\pi^-$ mass distribution. Lower curve is this distribution minus the ρ^0 distribution fitted to the overall dipion mass distribution, as described in the text. There are 79115 total dipion combinations and 16811 correlated combinations.

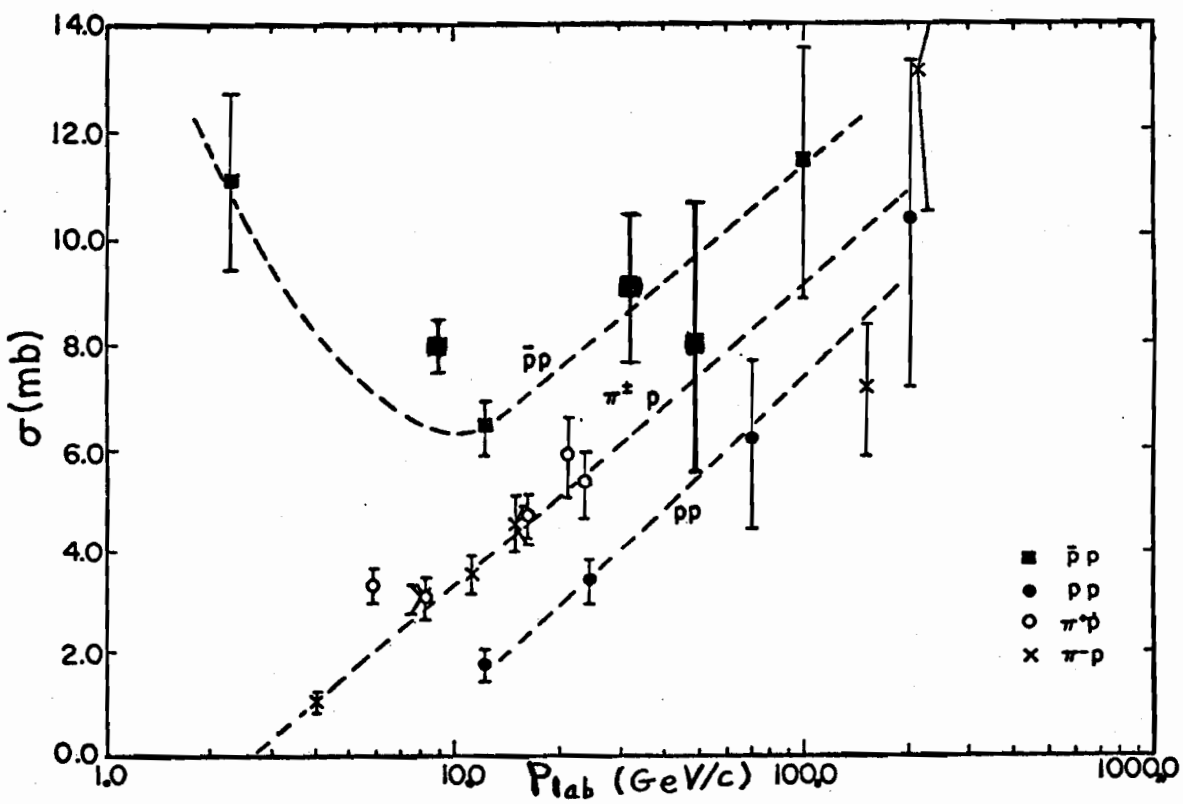

Fig. 33. From Ref. 65. Inclusive ρ^0 production cross sections as a function of p_{lab} for various beams incident on protons. Points at 9.1, 32, and 50 GeV/c have been added. Curves are to guide the eye.

I calculate a ratio $\rho^o/\pi^o = 0.13 \pm 0.023$. The FNAL-Cambridge-MSU group for 100 GeV/c quote a ratio of 0.125 ± 0.03. The Purdue 50 GeV data are shown in Figure 32, where the correlated $\pi^+\pi^-$ pairs[69] are plotted in toto and also with fitted ρ^o subtracted. The ρ^o fit was done using all $\pi^+\pi^-$ pairs, including uncorrelated pairs, with a background shape $e^{-bM_{\pi\pi}}$, and gives $\sigma(\rho^o) = 8.0 \pm 2.5$ mb, with reasonable mass and width $M_\rho = 757 \pm 11$ MeV and $\Gamma_\rho = 153 \pm 47$ MeV. It is noteworthy that after subtracting the ρ^o signal, a large number of correlated pairs remain. The $\pi^+\pi^-$ pairs resulting from $\omega^o \to \pi^+\pi^-\pi^o$ decay can account for a modest fraction of the remaining correlated signal: typically ρ^o and ω^o production are found to be comparable, in agreement with simple quark models. $K^{*\pm}$ production at 50 GeV is found to be small, and if K^{*o} production is comparable it can account for at most a small fraction of the correlated pairs (via unidentified $K^\pm$ treated as $\pi^\pm$). In conclusion, there is a substantial correlated $\pi^+\pi^-$ signal which is not associated with known vector mesons. Whether this signal is due to higher multiplicity resonances or to more general "clusters" is not known.

The ρ^o inclusive cross section is shown as a function of laboratory $\bar{p}$ momentum, in Figure 33, which is taken from Ref. 65 and to which I have added points at 9.1, 32, and 50 GeV/c. After a steep fall at low energies, this cross section is compatible with a logarithmic increase with energy, as are the cross sections for inclusive ρ^o production by $\pi^\pm$ or by protons.

Production of f^o is measured at 100 GeV[65] for large $p_T(\pi^+\pi^-) >$ 1 GeV/c, for which the inclusive f^o cross section is (1.2 ± 0.6)mb. The L-S group report at 9.1 GeV/c an inclusive f^o cross section (1.09 ± 0.15)mb for non-annihilation reactions (and 3.65 ± 0.22 mb for annihilations). However, the fitted f^o mass comes out rather high in both cases, about 1.31 GeV/c^2, indicating possible systematic effects in the treatment of the background shape.

9. Symmetries and a General Theorem

9.1 Beam-Target Reversal Symmetry

The Melbourne group have pointed out[70] that the G-parity operator

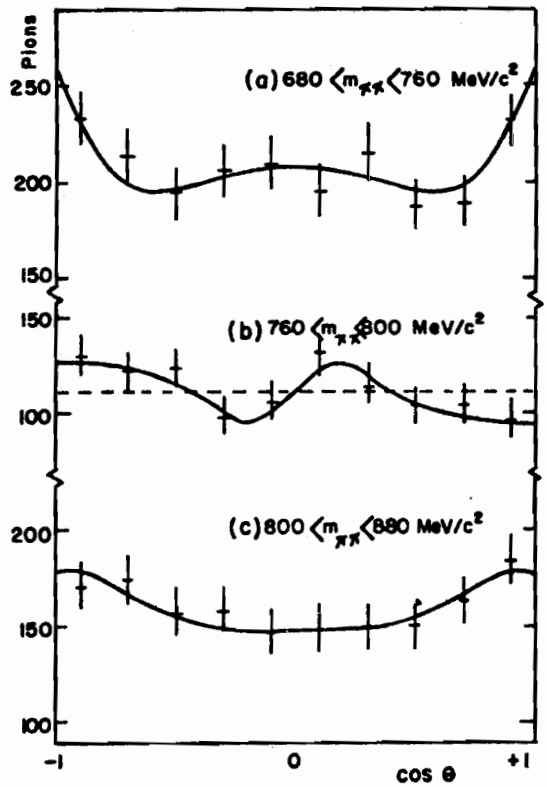

Fig. 34. From Ref. 70. Center-of-mass angular distributions for $\pi^+\pi^-$ in the ρ^o -ω^o overlap region and in two adjacent mass bins, from the reaction $pn \rightarrow \pi^+\pi^-\pi^-\pi^o$. Curves (a) and (c) are symmetric; curve (b) shows antisymmetry plus a flat background.

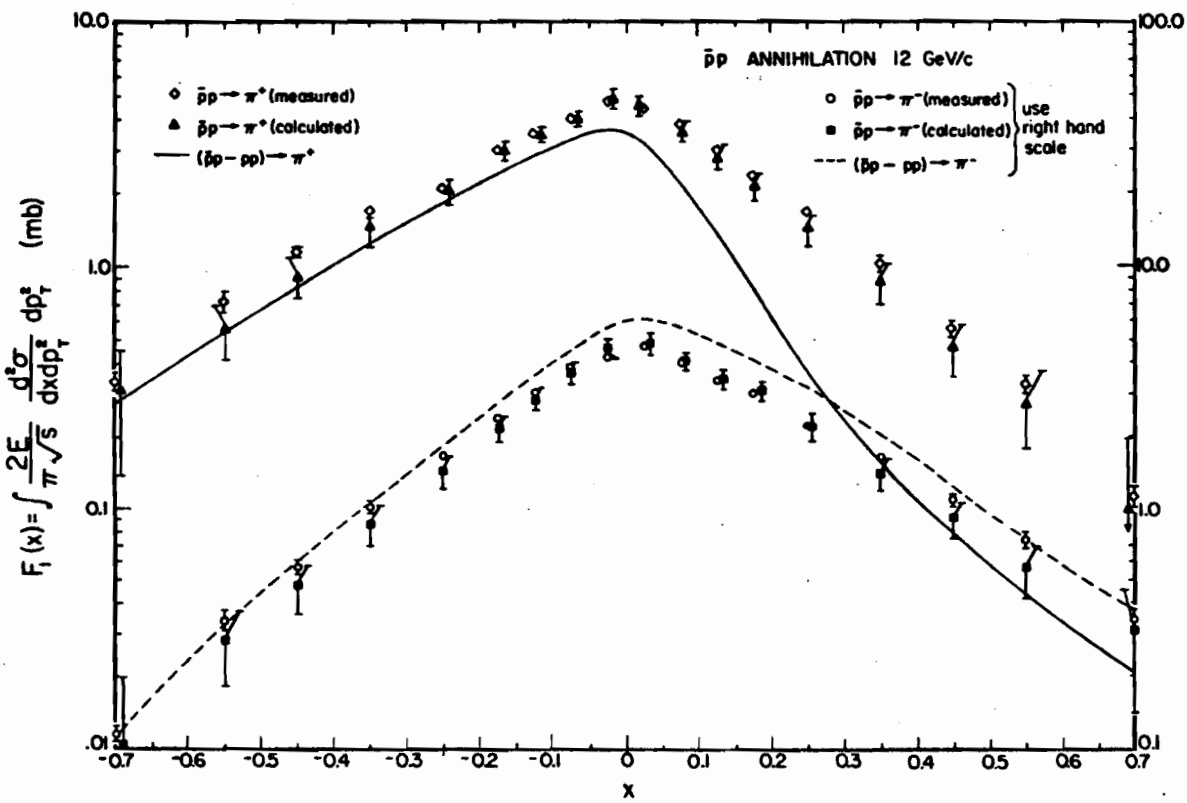

Fig. 35. From Ref. 75. "Comparison of explicit annihilation data at 12 GeV/c with predictions of the derived formulas. Note the different scales for the two sets of data. The curves are the prediction of the charge-symmetry-violating subtraction formulas."

applied to the system $\bar{p}_b n_t$ gives $n_b \bar{p}_t$ where the subscripts b and t refer to beam and target, respectively. Therefore any produced particles which are eigenstates of G will be distributed with forward-backward symmetry

$$\frac{d\sigma}{d\Omega}(\cos\theta) = \frac{d\sigma}{d\Omega}(-\cos\theta)$$

where θ is the center of mass polar angle with respect to the collision axis. Incident helicities have been averaged over, and the result applies to unpolarized beam and target. This symmetry should apply to inclusive as well as exclusive processes, although the authors test it specifically in certain annihilation channels, where the symmetry is well obeyed experimentally (to better than 4%) except in the region of the $(\rho^\circ - \omega^\circ) \to \pi^+\pi^-$ overlap where the G-violating $\omega^\circ \to 2\pi$ decay induces antisymmetry (Figure 34).

This symmetry, which is not present in the $\bar{p}p$ system, should be useful at high energies for studies of meson production in $\bar{p}n$ interactions, both inclusive and exclusive.

9.2 Tests of Charge Conjugation Invariance in the $\bar{p}p$ System

A sensitive test of C invariance in the $\bar{p}p$ system has been made by a Princeton-BNL group[71] at $\sqrt{s} = 5.44$ GeV. They compare the inclusive momentum distributions for positive and negative pions produced at 90° in the center of mass system, based on 5×10^9 antiprotons on target and 2×10^8 single-arm spectrometer triggers. The measured charge asymmetries $(N_+ - N_-)/(N_+ + N_-)$ are tabulated below, for various ranges of p_T, and are all consistent with zero.

P_T	0.5 - 0.6	0.6 - 1.0	1.0 - 2.7 GeV/c
$\frac{N_+ - N_-}{N_+ + N_-}$	0.002 ± .018	0.016 ± .015	0.001 ± .031

Average: 0.006 ± .009

The authors conclude that there is no statistically significant deviation from C-invariance. The resulting limit on a possible C-violating amplitude, α, is: $\mathrm{Re}(\alpha) \leq 0.0045$ relative to the C-conserving amplitude.

9.3 A General Theorem for Inclusive Hadronic Processes

A rather interesting and general theorem has been proved by Raja[72] and applied to 100 GeV $\bar{p}p$ interactions[73]. The theorem is based only on unitarity and crossing symmetry, and states that for an inclusive scattering process $a + b \rightarrow \bar{c} + X$ and for the semi-inclusive process $a + b \rightarrow \bar{c} + X_s$ where X_s is any subset of X, the ratios of invariant cross sections $f \equiv E\frac{d^3\sigma}{dp^3}$ are functions only of the mass M of X (and of X_s) and are not functions of s or t:

$$\frac{f(ab \rightarrow \bar{c} + X_s)}{f(ab \rightarrow \bar{c} + X)} = \frac{f(ac \rightarrow \bar{b} + X_s)}{f(ac \rightarrow \bar{b} + X)} = \frac{f(bc \rightarrow \bar{a} + X_s)}{f(bc \rightarrow \bar{a} + X)} = \alpha_s(M^2)$$

One consequence of these relations, for example, is that the mean multiplicity of a hadronic system X (integrated over t) is a function of M^2 only and not of s, a result which is well established experimentally[74].

Another consequence applies to the $\bar{p}p$ system, which has CP symmetry but whose inclusive charged particle distributions can contain both components which are even and odd under forward-backward reflection. This fact casts serious doubt on the use of a naive $\bar{p}p$ - pp subtraction procedure to estimate the charged particle inclusive distributions for the annihilation process (the pp system has only even components under reflection). However, the above theorem together with charge symmetry implies that the ratio of the odd to even parts of the annihilation component is everywhere equal to the same ratio for the non-annihilation component. From this relation follows a nonlinear formula for extracting the inclusive $\pi^{\pm}$ distributions for annihilations, using the overall $\bar{p}p$ and $pp \rightarrow \pi^{\pm}$ inclusive distributions. Raja has applied this method with striking success to 12 GeV data[75] where the annihilation component is also measured directly (Figure 35).

A further test[73] compares inclusive data with low multiplicity (2, 4 and 6 prong) and high multiplicity (12, 14 and 16 prong) subsets of the same data, and shows good scaling over a wide range of t and M^2.

Raja notes that the theorem is applicable to a wide variety of interactions, strong electromegnetic and perhaps weak; and that the relations so obtained severely restrict the possible shapes of particle

spectra[72]

10. Applications of the Quark Parton Model to "Soft" Hadronic Processes

While the quark jet fragmentation model has had some success in describing rare processes at large p_T, these models (with one notable exception to be discussed below) tend to fail in describing the bulk of inelastic hadron production which occurs at low p_T. An alternative approach, the quark recombination model[77,78,79,80] envisions a basic collision between one quark in the beam and one quark in the target. To form low p_T mesons in the baryon fragmentation region, for example, each of the remaining spectator valence quarks then picks up a co-moving soft ocean antiquark. The resulting meson has Feynman x equal to the sum of the valence quark and ocean quark momenta, and the model can in fact yield realistic cross sections for meson production in the beam and target fragmentation regions. Moreover, by counting types of spectator valence quarks and using a model of the valence quark distributions, it is possible to probe the ocean quark distributions, by fitting observed particle ratios such as π^+/π^-, K^+/K^-, K^o/π^+, as a function of x. Further particle ratios can also then be successfully predicted.

This model is suited to the non-annihilation part of $\bar{p}p$ scattering, as well as to other inelastic hadronic scattering in general. This model has been applied, for example, with considerable success to pp scattering at 100 to 400 GeV/c by Duke and Taylor[80] who successfully predict particle ratios and who find the quark ocean concentrated at small x, as usual. However, they reach the startling conclusion that valence plus ocean quarks saturate the quark momentum sum rule for the proton, unlike the well-known quark distributions sampled by lepton-hadron scattering which account for only 50% of the momentum carried by the proton. The other 50% is conventionally assumed to be carried by neutral vector gluons. The authors speculate that during the time of the recombination process essentially all gluons have dissociated into quark-antiquark pairs which contribute to the effective ocean.

The recombination model has also been successfully applied to 360 GeV/c π^-p scattering by a Michigan State-Iowa State-Maryland-Notre Dame collaboration[81] who study the inclusive reactions $\pi^-p \rightarrow a + b + X$ where the "trigger" particle, a, is $K^o = (d\bar{s})$, $\pi^+ = (u\bar{d})$ or $\pi^- = (d\bar{u})$,

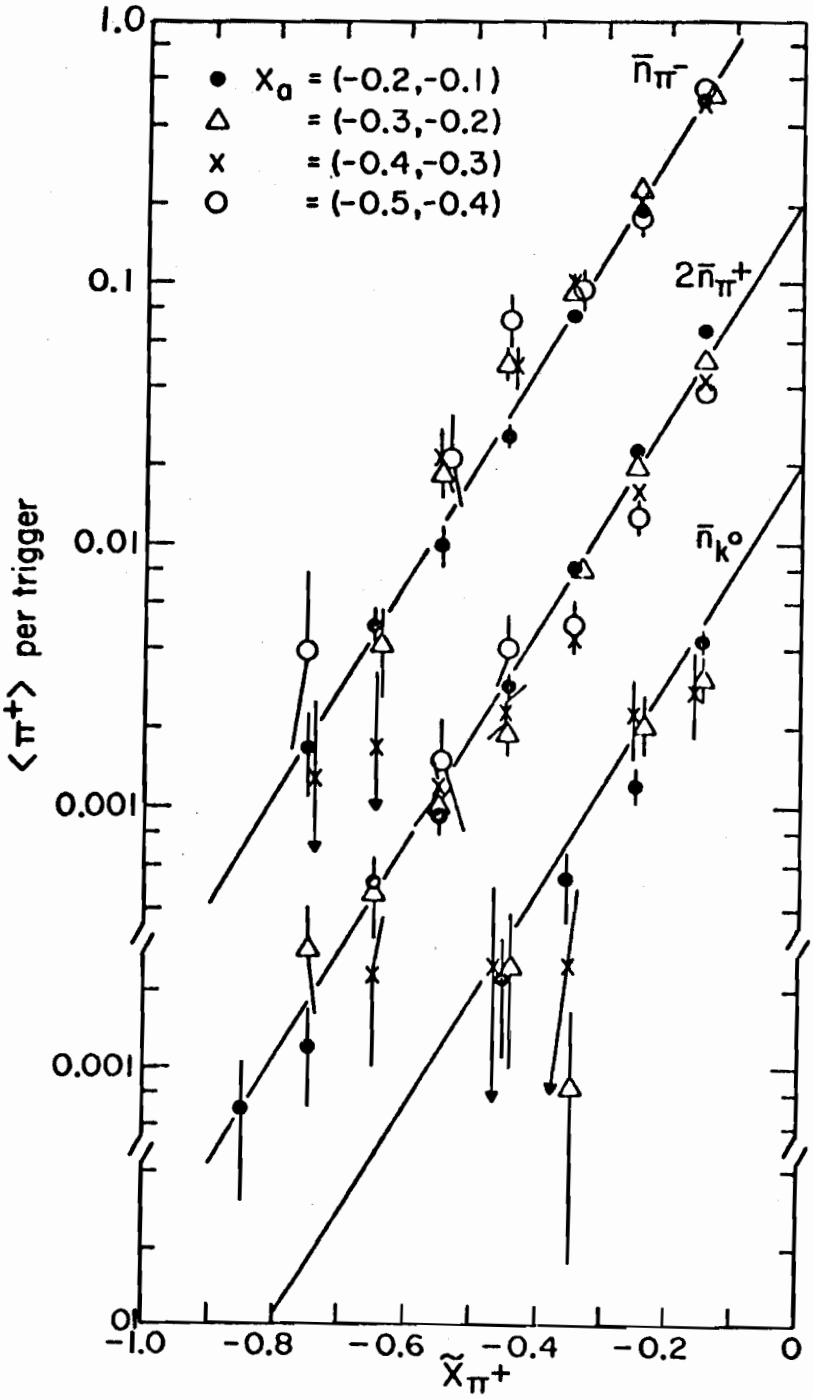

Fig. 36. From Ref.81. The average π^+ multiplicity per trigger particle as a function of $x_b = x_{\pi^+}$ for various values of x_a, for trigger particles π^-, K^0, and π^+. The π^+ trigger data are multiplied by 2. A common line with the same slope and absolute normalization is compared to each of the three triggers.

and where the second particle, b, is a π^+. In the target proton fragmentation region, one expects particle b to scale in terms of the variable $\tilde{x}_b = x_b/(1-x_a)$, the ratio of the longitudinal momentum b to its maximum value. The scaling distribution of b = π^+ per trigger particle is shown in Figure 36 where the distribution for trigger π^+ is multiplied by two. One of the valence u quarks is eaten by the trigger π^+ while both valence u quarks are left when the trigger particle is a K^o or a π^-. The distributions scale well in $\tilde{x}_b$, for a variety of values of x_a. The ratios of these curves for the three trigger particles are $\bar{n}_{\pi^-}/\bar{n}_{K^o} \sim 1.3$ and $\bar{n}_{\pi^-}/2\bar{n}_{\pi^+} \sim 1.7$. The departures of these ratios from unity can be explained by a limited average number of ocean quarks, in the range $\sim$ 2 to 3. Then the ocean quark eaten by the trigger particle is not available to form particle b, and the authors predict by simple combinatorics that $\bar{n}_{\pi^-} = \frac{2m}{2m-1}(\bar{n}_{K^o}) = \frac{m}{m-1}(2\bar{n}_{\pi^+})$, where m is the mean number of ocean quarks. The corresponding values of m, 2.2 and 2.4 are consistent with each other and with the authors' expectations for the ocean quarks.

An alternative to the quark recombination model is the quark fragmentation model as applied by Andersson, Gustafson and Peterson[82] to the meson (or baryon) fragmentation regions (but avoiding that part due to diffractive dissociation of beam or target). The crucial ansatz of these authors is that the interacting valence quarks prefer to be at small Feynman x, and hence the spectator quark (or diquark) will carry a large fraction of the original hadron's momentum. The authors motivate this ansatz by reference to the properties of Quantum Chromodynamics where the gluon-quark coupling increases for low momentum transfers. The salient feature of this picture is that the quark distributions inside the hadrons are different immediately after the strong quark-quark interaction, and are not given by the quark distributions as probed by lepton-hadron scattering. In particular, since the quark distribution function is approximately proportional to $\delta(1-x_F)$, then to find the probability:

$$\frac{1}{\sigma}\frac{d\sigma}{dx_F} \equiv F^{H \to h}(x_F)$$

that incoming hadron H produces a hadron of type h at $p_{11}/p_{11}^{max} \equiv x_F$, the usual convolution integral over the quark distribution functions and the

quark fragmentation functions can be replaced approximately by:

$$F^{H \to h}(x_F) = D^*(x_F)$$

where $D^*(x_F)$ is an appropriate linear conbination (depending on beam, target and produced hadron[82]) of the quark fragmentation functions D_q^h defined by Field and Feynman[83]. Reasonable agreement is obtained between D_q^h measured in leptoproduction, and distributions of produced pions in the reactions $\pi^{\pm}p \to \pi^{\pm} X$ or $\pi^{\mp} X$ at 100 GeV, both for $0.2 \leq x_F \leq 0.9$ in the pion fragmentation region and for $-0.5 \leq x \leq -0.2$ in the proton fragmentation region. Agreement is also found for photoproduction in the photon fragmentation region, when the diffractive $\gamma \to \rho^o$ portion is removed. And agreement is found for the reactions $K^-p \to \pi^+ X$ at 32 GeV/c and $\pi^-p \to K_s^o X$ at 18.5 and 250 GeV/c, all in the meson fragmentation region.

It will be interesting to study further consequences of these two models, quark fragmentation vs. quark recombination, to establish domains of validity and to see where further refinements are necessary.

Acknowledgements

I thank my colleagues at Purdue, and particularly D.E. Zissa, L.K. Rangan, and E. Fernandez, for their contributions to the analysis of the 50 GeV/c $\bar{p}p$ data.

REFERENCES

1. A.S. Carroll, et al., Phys. Lett. 61B, 303 (1976).
2. J. Whitmore, Particles and Fields (APS/DPF Seattle, 1975) p. 236.
3. Y. Eylon and H. Harari, Nucl. Phys. B80, 349 (1974).
4. J.G. Rushbrooke, et al., Phys. Lett. 59B, 303 (1975).
5. CERN-Pisa-Rome-Stony Brook Collaboration, Phys. Lett. 62B, 460 (1976).
6. R.E Hendrick, et al., Phys. Rev. D11, 536 (1975).
7. H.J. Lipkin, Phys. Rev. D17, 366 (1978); Phys. Rev. D11, 1827 (1975); Nucl. Phys. B78, 381 (1974); Phys. Lett. 56B, 76 (1975).
8. S.P. Denisov, et al., Nucl. Phys. B65, 1 (1973).
9. A. Hacinliyan and M. Koca, Phys. Rev. D13, 1868 (1976).
10. G.F. Chew and C. Rozenzweig, Phys. Lett. 58B, 93 (1975); Phys. Rev. D12, 3907 (1975).
11. P.R. Stevens, G.F. Chew and C. Rosenzweig, Nucl. Phys. B110, 355 (1976).
12. D.W. Duke, Phys. Lett. 71B, 342 (1977).

13. E. Eisenhandler, et al., Nucl. Phys. B113, 1 (1976).
14. J.S. Russ, et al., Phys. Rev. D15, 3139 (1977).
15. C. Bruneton, et al., Nucl. B124, 391 (1977).
16. C.W. Akerlof, et al., Phys. Rev. D14, 2864 (1976).
17. D.S. Ayres, et al., Phys. Rev. D15, 3105 (1977); Phys. Rev. D14, 3092 (1976).
18. H. DeKerret, et al., Phys. Lett. 62B, 363 (1976).
19. J.L. Hartman, et al., Phys. Rev. Lett. 39, 975 (1977).
20. L. VanHove, Nucl. Phys. B122, 525 (1977).
21. Fermilab Single Arm Spectrometer Group. Phys. Rev. Lett. 37, 548 (1976).
22. "Hadron Elastic Scattering-An Experimental Review", J. Lach, Fermilab-Conf-77/38-EXP and references therein.
23. L. VanHove, Rev. Mod. Phys. 36, 655 (1964).
24. M. Bishari, Phys. Lett. 66B, 54 (1977).
25. J. Dias de Deus, Nucl. Phys. B59, 231 (1973); A.J. Buras and J. Dias de Deus, Nucl. Phys. B71, 481 (1974).
26. V. Barger and R.J.N. Phillips, Nucl. Phys. B97, 452 (1975).
27. R.E. Hendrick and B. Lautrup, Phys. Rev. D11, 529 (1975).
28. U. Almaldi, et al., Phys. Lett. 66B, 390 (1977).
29. E. Jenkins, et al., Fermilab-Pub-78-35 EXP.
30. P. Jenni, et al., Nucl. Phys. B129, 232 (1977).
31. P. Soding, Phys. Lett. 8, 285 (1964); W. Grein, Karlsruhe University Report TKP 77-4 (March, 1977); Nucl. Phys. B131, 255 (1977).
32. M.D. Corcoran, et al., Phys. Rev. Lett. 40, 1113 (1978).
33. J. Pumplin and G.L. Kane, Phys. Rev. D11, 1183 (1975).
34. M.G. Albrow, et al., Nucl. Phys. B108, 1 (1976).
35. R. Blankenbecker and S.J. Brodsky, Phys. Rev. D10, 2973 (1974); S.J. Brodsky and G.R. Farrar, Phys. Rev. Lett. 31, 1153 (1973); Phys. Rev. D11, 1309 (1975), Sivers, et al., Phys. Rep. 23C,1 (1976).
36. Y. Akimov, et al., Phys. Rev. Lett. 39, 1432 (1977).
37. D. Denegri, et al., Nucl. Phys. B114, 413 (1976).
38. G. Goggi, et al., Phys. Lett. 72B, 261 (1977).
39. M. Cavalli-Sforza, et al., Nuovo Cimento Lett., 14, 345, 353, 359 (1975).
40. G.C. Mantovani, et al., Phys. Lett. 65B, 401 (1976).
41. S.Y Chu, et al., Phys. Rev. D13, 2967 (1976); C. Pajares and R. Pascual, Phys. Rev. D14, 258 (1976); and Phys. Rev. D16, 1359 (1977); W.R. Frazer and F.E. Paige, Phys. Rev. D16, 913 (1977).
42. H. Miettinen and J. Pumplin, Fermilab-Pub-78/21-THY(February,1978).
43. J. Pumplin, Phys. Rev. D8, 2899 (1973).
44. L. VanHove and K. Fialkowski, Nucl. Phys. B107, 211 (1976); and Ref. 20.
45. H. DeKerret, et al., Phys. Lett. 69B, 372 (1977).
46. G. Goggi, et al., Phys. Lett. 72B, 265 (1977).
47. A. Bouquet and B. Diu, Nuovo Cimento Lett. 20, 463 (1977).
48. B. Diu and A. Ferraz de Carmargo, Nuovo Cimento Lett. 20, 609 (1977).
49. R.L. Anderson, et al., Phys. Rev. Lett. 38, 880 (1977); Phys. Rev. Lett. 37,1111 (1976); D.S. Ayres, et al., Phys. Rev. Lett. 37, 1724 (1976).

50. E.W. Beier, et al., Phys. Rev. Lett. 37, 1120 (1976).
51. G.W. VanApeldoorn, Nucl. Phys. B133, 245 (1978).
52. R. Stenbacka, et al., Nucl. Phys. B131, 386 (1977).
53. H.W. Atherton, et al., Nuovo Cimento Lett. 30A, 505 (1975).
54. P.S. Gregory, et al., Nucl. Phys. B119, 60 (1977).
55. M.A. Jabiol, et al., Nucl. Phys. B127, 365 (1977).
56. Yu.M. Antipov, et al., Nucl. Phys. B99, 189 (1975).
57. Ch. Walck, et al., Nucl. Phys. B100, 61 (1975).
58. R. Raja, et al., Phys. Rev. D15, 627 (1977); D.R. Ward, et al., Phys. Lett. 62B, 237 (1976).
59. D. Bertrand, et al. Nucl. Phys. B128, 365 (1977).
60. S.M. Jacobs, et al., Phys. Rev. D17, 1187 (1978).
61. G. Plaut, Nucl. Phys. B35, 221 (1971).
62. J. Whitmore, Phys. Reports 27C, 187 (1976).
63. F.T. Dao and J. Whitmore, Phys. Lett. 46B, 252 (1973).
64. D. Cohen, Phys. Lett. 47B, 457 (1973).
65. R. Raja, et al., Phys. Rev. D16, 2733 (1977).
66. R. Singer, et al., Nucl. Phys. B135, 2 (1978).
67. G. Jansco, et al., Nucl. Phys. B124, 1 (1977).
68. See Ref. 55. If one assumes that these are 0.7 protons and 0.7 antiprotons per inelastic event, then the average number of π^- is equal to the quoted average number of π^0.
69. The uncorrelated background was obtained by pairing π^+ from one event with π^- from other randomly selected events. For a discussion of two particle correlations in terms of the mass variable, see E.L. Berger, R. Singer, G.H. Thomas and T. Kafka , Phys. Rev. D15, 206 (1977).
70. E. Gold, et al., Phys. Rev. D16, 2679 (1977).
71. R. Cester, et al., Phys. Rev. D17, 1706 (1978).
72. R. Raja, Fermilab-Pub-77/28-EXP(1977).
73. R. Raja, Fermilab-Pub-77/29-EXP(1977).
74. J. Whitmore, Phys. Rep. 10C, 273 (1974).
75. R. Raja, Phys. Rev. D16, 142 (1977).
76. M. Della Negra, et al., Phys. Lett. 65B, 394 (1976).
77. W. Ochs, Nucl. Phys. B118, 397 (1977).
78. K.P. Das and R.C. Hwa, Phys. Lett. 68B, 459 (1977).
79. T.A. DeGrand and H.I. Miettinen, Phys. Rev. Lett. 40, 612 (1978).
80. D.W. Duke and F.E. Taylor, Fermilab-Pub-77/95-THY (1977).
81. E. Lehman, et al., presented at the IX International Symposium on High Energy Multiparticle Dynamics, Tabor, Czechoslovakia (July, 1978).
82. B. Andersson, G. Gustafson, and C. Peterson, Phys. Lett. 69B, 221 (1977); Phys. Lett. 71B, 337 (1977).
83. R.D. Field and R.P. Feynamn, Phys. Rev. D15, 2590 (1977).